DOT/FAA/CT-90/14

FAA Technical Center
Atlantic City International Airport
N.J. 08405

Decision-Height Windows for Decelerating Approaches in Helicopters—Pilot/Vehicle Factors and Limitations

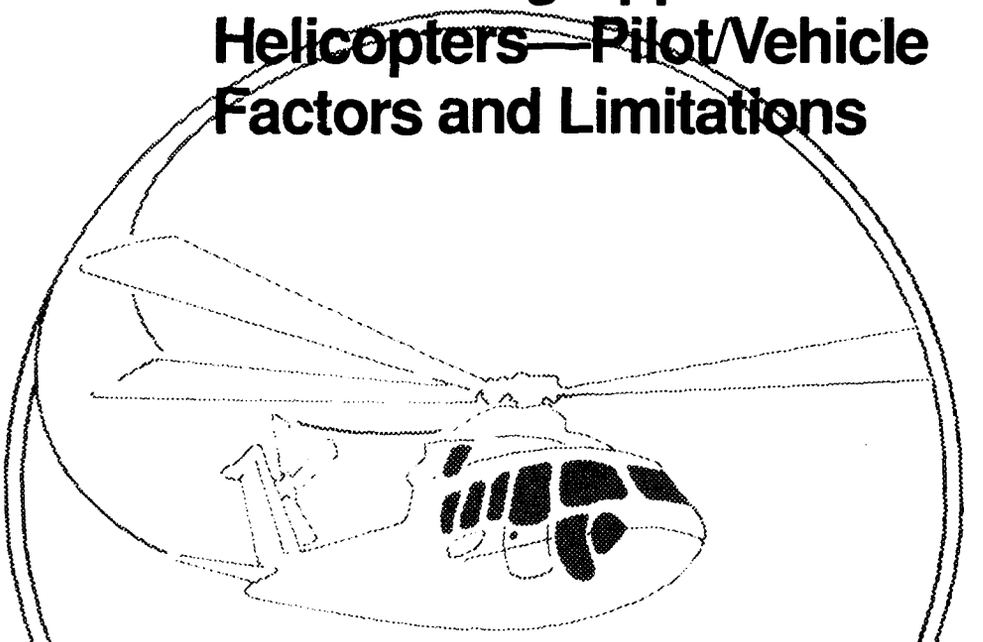

April 1991

Final Report

U.S. Department of Transportation
Federal Aviation Administration

NOTICE

This document is disseminated under the sponsorship of the U. S. Department of Transportation in the interest of information exchange. The United States Government assumes no liability for the contents or use thereof.

The United States Government does not endorse products or manufacturers. Trade or manufacturers' names appear herein solely because they are considered essential to the objective of this report.

Technical Report Documentation Page

1. Report No.	2. Government Accession No.	3. Recipient's Catalog No.
DOT/FAA/CT-90/14		

4. Title and Subtitle	5. Report Date
DECISION-HEIGHT WINDOWS FOR DECELERATING APPROACHES IN HELICOPERS--PILOT/VEHICLE FACTORS AND LIMITATIONS	April 1991
	6. Performing Organization Code
7. Author(s)	8. Performing Organization Report No.
R.H. Hoh, S. Baillie, S. Kereliuk, and J.J. Traybar	DOT/FAA/CT-90/14
9. Performing Organization Name and Address	10. Work Unit No. (TRAIS)
Systems Control Technology Inc. 1611 N. Kent Street, Suite 910 Arlington, VA 22209	11. Contract or Grant No. Work Order 5E DTFA-01-87-C-00014
	13. Type of Report and Period Covered
12. Sponsoring Agency Name and Address U.S. Department of Transportation Federal Aviation Administration Technical Center Atlantic City International Airport, NJ 08405	Final Report Jan. 1989 - May 1991
	14. Sponsoring Agency Code ACD-230

15. Supplementary Notes

R.H. Hoh, HOH Aeronautics Inc. S. Baillie, and S. Kereliuk
J.J. Traybar (COTR) FAA National Research Council-Canada

16. A combined analysis and flight test program was conducted to investigate the characteristics of the decision-height (DH) window for helicopter decelerating instrument approaches. The concept of an effective flight path angle has been employed to define the DH window in terms of basic rotorcraft performance data. Exploratory flight tests were conducted to validate this approach and to define the approximate dimensions of the DH window 50 feet above ground level. The flight test experiment included an instrument meteorological conditions (IMC) decelerating instrument approach with errors built into the flight director to cause the helicopter to arrive at the decision-height with some glideslope and groundspeed errors. The pilots were required to visually maneuver the rotorcraft from decision-height to a steady hover over the helipad. The decision-height window was formulated on a grid of glideslope error versus the groundspeed at decision-height. The results indicate that the high speed boundary of the DH window is a function of the minimum usable torque, and related to maximum acceptable pitch attitude during deceleration. Some margin is required to account for pilot delay or control misapplication after breakout. The upper glideslope error boundary is based on the maximum negative aerodynamic flight path angle that can be flown at low airspeeds. Poor visual cuing after breakout tends to emphasize the need for margins from the helicopter performance. The low speed boundary of the DH window is based on rotorcraft handling qualities at very low airspeeds. The low glideslope boundary is dependent on obstruction avoidance and ability to see the heliport environment upon breakout at decision-height.

17. Key Words	18. Distribution Statement
Helicopter Data Instrument/Heliport Approaches Decision-Height Controls/Displays/Flying Qualities	Document is available to the public through the National Technical Information Service, Springfield, Virginia 22161

19. Security Classif. (of this report)	20. Security Classif. (of this page)	21. No. of Pages	22. Price
Unclassified	Unclassified	63	

Form DOT F 1700.7 (8-72) Reproduction of completed page authorized

PREFACE

This research was accomplished under the auspices of a Memorandum of Agreement between the Federal Aviation Administration (FAA Technical Center) and the National Research Council (NRC) Flight Research Laboratories, Ottawa, Canada. The work reported herein was performed under contract to Systems Control Technology (SCT) Inc., Arlington VA and under subcontracts to Hoh Aeronautics Inc., (HAI) Lomita, CA and the Starmark Corporation, Arlington, VA.

Hoh Aeronautics Inc. provided pre-experimental analysis and planning, and on-site flying and data interpretation, while both HAI and Starmark participated with the FAA, NRC, and SCT in technical reviews. The interpretation and analysis of the flight test data presented herein, and the preparation and production of this report was accomplished by Hoh Aeronautics Incorporated. The NRC Flight Research Laboratories set up and conducted the experiments using their Bell-205A airborne research helicopter, ancillary ground facilities and data reduction equipment, and provided engineering analysis and data interpretation throughout all phases of the work. The NRC report covering these activities is given as Reference 3 of this report.

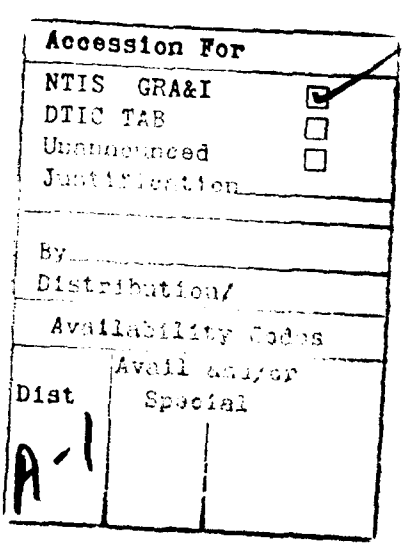

TABLE OF CONTENTS

LIST OF FIGURES

LIST OF SYMBOLS AND ABBREVIATIONS

AFCS	Automatic flight control system
AGL	Above ground level
a_x	Acceleration along x axis (flight path vector)
DH	Decision height
$d\epsilon$ or DEPS	Glideslope error (see Figure 1)
FAA	Federal Aviation Administration
g	Gravity (32.2 ft/sec^2)
h	Altitude above ground
HOV	Hover
HQR	Cooper Harper Handling Quality Rating from the Figure 6 scale
IFR	Instrument flight rules
IMC	Instrument meteorological conditions
IGE	In ground effect
kts	Knots
MLS	Microwave landing system
NASA	National Aeronautics and Space Administration
NRC	National Research Council, Canada
NWGAMAEFF	Effective flight path angle (see Figure 3), calculated without the effect of wind
psi	Pounds per square inch
R	Range along axis parallel to horizon from DH point to hover
R_s	Slant range from DH point to hover
STOL	Short takeoff and landing

t	Time
TERPS	Terminal instrument procedures
u	Component of velocity along x axis
V or V_{GS}	Groundspeed - Velocity with respect to the ground
V_a	Airspeed - Velocity with respect to the airmass
V_{wind}	Speed of wind parallel to horizon - positive for a tailwind
V_I	Velocity with respect to an inertial coordinate system
V_{DH}	Groundspeed at decision-height
VMC	Visual meteorological conditions
γ	Flight path angle - angle of velocity vector with respect to horizon
γ_{aero} or γ_a	Aerodynamic flight path angle - flight path angle with respect to the wind (see Figure B-1)
γ_{eff} or GAMAEFF	Effective flight path angle (see Figure 3)
γ_f or GAMAF	Geometric flight path angle from rotorcraft position at DH to hover point
$\gamma_{inertial}$ or γ_I	Inertial flight path angle - flight path angle with respect to earth fixed coordinates
γ_o or GSANGLE	Angle of electronic glideslope
δ_{col}	Deflection of the collective controller
δh	Change in altitude
θ	Rotorcraft pitch attitude with respect to the horizon
w	Component of velocity along z axis - positive down

EXECUTIVE SUMMARY

A combined analysis and flight test program was conducted to investigate the characteristics of the decision-height (DH) window for helicopter decelerating instrument approaches. The concept of an effective flight path angle has been employed to define the DH window in terms of basic rotorcraft performance data. Exploratory flight tests were conducted to validate this approach and to define the approximate dimensions of the DH window for a Bell 205A with rate augmentation for a decision-height of 50 ft above ground level. The flight test experiment included an IMC decelerating instrument approach with errors built into the flight director to cause the helicopter to arrive at the decision-height with some glideslope and groundspeed errors. The pilots were required to visually maneuver the rotorcraft from decision height to a steady hover over the helipad.

This program only considered the limitations due to piloted control of the rotorcraft from DH to hover. Other limitations, such as obstruction avoidance while still in IMC conditions, should be superimposed on these results. For example, the allowable glideslope tracking error for obstruction avoidance will probably be calculated based on formulas similar to those used for current terminal instrument procedures (TERPS). These are typically based on some multiple (usually 6) of the standard deviation of flight technical error, calculated from numerous approaches. Such numbers are available for shallow approaches, typical of fixed-wing aircraft, but need to be developed for the steeper approaches expected for rotorcraft into urban areas. Once they are calculated, they should be compared to the allowable error based on the pilot's ability to safely decelerate to hover as addressed herein. The smaller value sets the size of the DH window.

The decision-height window was formulated on a grid of glideslope error vs. the groundspeed at decision-height. The results indicate that the high speed boundary of the DH window is a function of the minimum usable torque and related maximum acceptable pitch attitude during deceleration. Some margin is required to account for pilot delay or control misapplication after breakout. The upper glideslope error boundary is based on the maximum negative aerodynamic flight path angle that can be flown at low airspeeds. Poor visual cuing after breakout tends to emphasize the need for margins from the helicopter performance. The low speed boundary of the DH window is based on rotorcraft handling qualities at very low airspeeds. The low glideslope boundary is dependent on obstruction avoidance, and ability to see the helipad environment upon breakout at DH.

I INTRODUCTION AND BACKGROUND

This program was conducted to define the basic limitations of the pilot plus rotorcraft in making the transition from a very low decision height (DH) to a steady hover over the helipad. The term "decision-height window" is defined herein as the limits of glideslope/localizer tracking errors and groundspeed variations, that can exist at breakout to allow a safe visual transition to hover. Such a window is required as a basis for defining TERPS boundaries for decelerating approaches and for setting autopilot coupler and flight director performance standards for decelerating instrument approaches in rotorcraft.

There have been several FAA and NASA experiments conducted to investigate tracking accuracy for helicopter instrument, and visual approaches, e.g., see Refs. 1 and 2. However, this work is the first to consider the required tracking and speed tolerances (i.e. "window") for decelerating instrument approaches to a very low decision height (50 ft above ground level (AGL)).

There are a wide variety of factors that must be considered in the determination of the dimensions of a decision-height window, e.g.,

- Rotorcraft flight dynamics limits.
- Limitations associated with the human pilot.
- Rotorcraft field-of-view
- Availability of airspace.
- Available real estate for the helipad, and approach lighting.
- Rotorcraft performance for a missed-approach

This study is concerned with the first two factors noted above. It is intended that the results of this study will be superimposed on the other considerations for the determination of a decision-height window for a given set of conditions consisting of rotorcraft performance limits, MLS configuration, and helipad geometry.

The research consisted of an analysis phase to determine the dimensions of the decision-height window based solely on rotorcraft performance. A flight test phase followed to determine the necessary margins that must be applied to the rotorcraft performance limits to account for limitations associated with the human pilot.

This work was done in the context of an exploratory study to determine what factors are important, and to obtain a general idea of the order of magnitude of the dimensions of the decision-height window. Further testing should be conducted to determine the effects of different rotor

configurations, helipad geometry and lighting, rotorcraft field-of-view, glideslope angle, and a more detailed look at the effects of winds. The testing focused primarily on the longitudinal axis and further work to determine the maximum allowable lateral offsets should be accomplished.

The test aircraft was the Institute for Aerospace Research, National Research Council (NRC) Canada's variable stability Bell 205A-1 Airborne Simulator, and all testing was conducted at the NRC facility in Ottawa Canada. The variable stability system is a full authority fly-by-wire, digital flight control system. Simulation of a degraded visual environment and IMC conditions was accomplished using an IMC Simulator manufactured by Instrument Flight Research Incorporated, Colombia, SC. This "simulator" consists of goggles with lenses that incorporated liquid crystals to vary the lens opacity. The goggles were wired to the airborne simulator's radar altimeter and set to clear at the 50 foot decision-height. Additional details regarding the facilities used in this experiment, as well as a presentation and analysis of the data, are contained in Reference 3; a report published by the NRC.

The report is organized as follows. The analysis phase of the work is presented in Section II, and indicates how rotorcraft performance can be interpreted to define certain boundaries of the decision-height window. The intent of this section is to present certain fundamental concepts as an aid to interpreting the flight test data, and detailed derivations are deferred to Appendix B. An overview of the experimental scenario is given in Section III, along with the results of exploratory runs to investigate the gross effects of several phenomena (e.g., fog after breakout, pad markings, and transition from manual vs. coupled approaches). The detailed results, and interpretations of those results, are presented in Section IV. These are further refined in Section V, where some example decision-height windows are defined. These are, of-course, based only on the pilot/vehicle considerations. Superimposing other constraints (such as noted above) could further reduce the size of the window. The effect of varying the glideslope angle, and the rotorcraft configuration (i.e., performance capability) is also presented in Section V. A summary of the key conclusions of the study are presented in Section VI. The basic data from the flight test experiment is presented in Appendix A in a spread sheet format, along with excerpted pilot commentary. This information is supplied to allow alternative analyses and interpretations by the reader. A derivation of the effective flight path angle parameter is given in Appendix B.

II FUNDAMENTAL CONSIDERATIONS

A. Approach Geometry

The nature of the approach geometry for very low decision-heights is such that glideslope errors can result in significant differences in the range to the hover point from breakout, as illustrated in Figure 1. Here it can be seen that a high approach results in a steeper visual segment (defined by γ_f in Figure 1). This can be alleviated by increasing the hover altitude, but possibly at the expense of losing the helipad under the nose, or risking reentry into cloud and a missed approach. In this program, the nominal glideslope angle (γ_o) was 9^o, the decision height was set at 50 ft, and the hover height was 10 ft, resulting in a nominal final segment (γ_f) of 7.2^o.[1] If the pilot is below glideslope at breakout, the flight path angle of the final segment (γ_f) will be more shallow than the reference 7.2^o. Steep approaches

[1] All of the glideslope angles in this study are negative. The sign of these angles has been dropped in the text and figures as a matter of convenience. Also, reference to greater or steeper values of glideslope angle are intended to refer to more negative values.

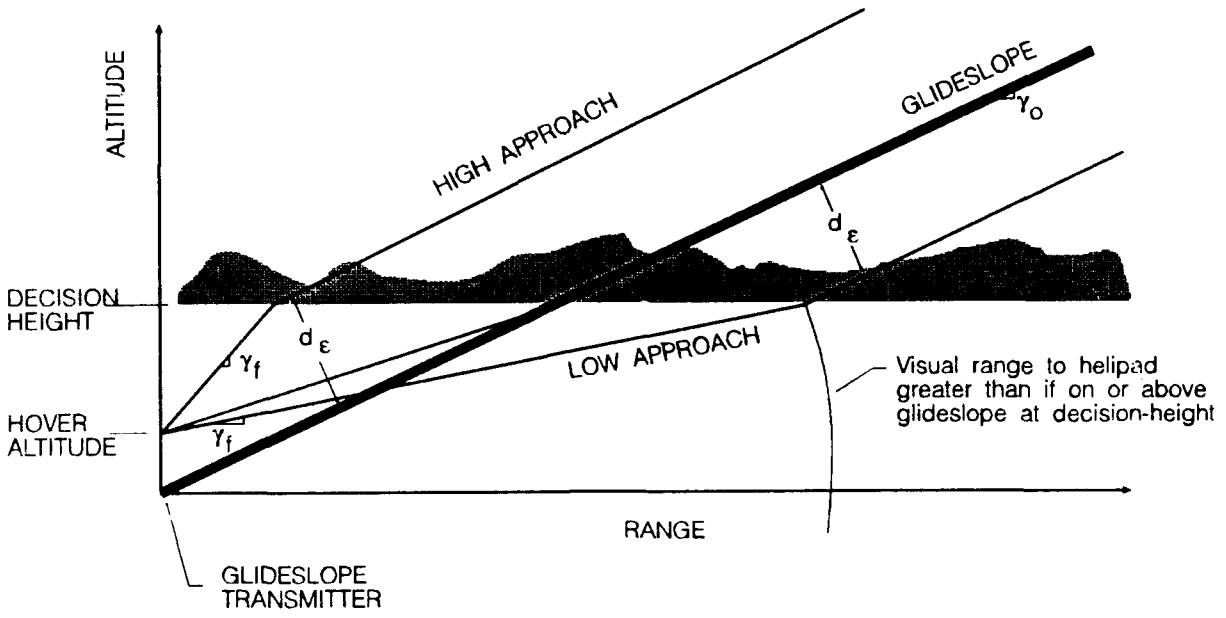

Figure 1. Approach Geometry - Decision-Height to Hover

are more critical from the standpoint of flight dynamics, and shallow approaches are critical in terms of helipad sighting at breakout, or collisions with obstructions. This program was focused primarily on the flight dynamics issue, and hence concentrated on the problem of being high and/or fast.

The decision point has been based on altitude as a matter of convention, however an alternative would be to base the decision point on range. This could have the effect of causing all high approaches to be missed. That is, the helicopter would still be in the clouds if high on glideslope, and if the "decision range" was set at the nominal glideslope at a reference altitude, say 50 ft. On that basis, and on the basis that there is no obvious advantage for using range as the decision point, the conventional decision-height definition was retained.

The decision-height window in Figure 1 has been defined as perpendicular to the glideslope. For "shallow" glideslopes (say less than 20°), it does not matter whether the window is perpendicular to the ground or to the glideslope. However, as the glideslope becomes steeper, this effect takes on additional significance, and must be properly accounted for. The glideslope error measurements made during the testing were perpendicular to the ground, however it is recommended that for steeper glideslopes, the error signals be perpendicular to the beam. For existing MLS systems, the system of measurement is in a $\rho - \theta$ coordinate system, and glideslope errors are easily resolved as perpendicular to the beam (i.e., $d_\epsilon = R \sin\theta$).

B. Relationships Between Decision-Height Window and Helicopter Performance Limits.

Helicopter performance limits that can have an effect on the transition from decision height to hover are:

1. Insufficient deceleration capability without entering autorotation.

2. The restricted height-velocity envelope for single engine rotorcraft.

3. Settling with power, or vortex ring state.

4. Degraded handling due to excessively low airspeed resulting in transition in and out of translational lift.

These are illustrated in Figure 2, on a generic decision-height window. The shape of the upper boundary of this window indicates a tradeoff between groundspeed and glideslope error. This is a result of the first of the above factors, which infers a limit on the ability of the rotorcraft to dissipate energy. The total energy is the sum of potential energy (Δh), and kinetic energy (V^2), so that a tradeoff exists between groundspeed, and glideslope error at breakout.[2]

Height-velocity problems could occur for a breakout at low airspeed and a high-on-glideslope condition (i.e. large value of γ_f). This condition would be most likely if there were a tailwind at breakout. Even if the rotorcraft is not in the height-velocity envelope, a close proximity to this condition may be limiting from a piloting standpoint.

The potential for steep approach angles dictates that the vortex-ring state issue be addressed, as illustrated in Figure 2. The sketch in Figure 2 is taken from the full-scale rotor data in Ref. 4, which indicates that ring-vortex encounters require a flight path angle of 30^{O} or greater.[3] Actually, it is the angle-of-attack of the rotor that is fundamentally limiting, and the interpretation in terms of flight path angle assumes a nearly level pitch attitude, and that the flight path angle is with respect to the airmass (i.e. the "aerodynamic" flight path angle). It follows that the most critical condition would be a breakout high on the glideslope and in a tailwind. The relationship between the aerodynamic and inertial flight path angles is,

$$\tan\gamma_{aero} = \tan\gamma_{inertial}\left(1 + \frac{V_{wind}}{V_{airspeed}\cos\gamma_{aero}}\right)$$

---

[2] Groundspeed is used because it is, by definition, zero at hover. Therefore, any groundspeed that exists at breakout must be dissipated at the hover point or an overshoot will occur.

[3] The edge of the vortex ring region involves some recirculation of air through the rotor plane. This shows up as increased vibration, but with little accompanying loss of performance. Proceeding deeper into the vortex-ring region involves recirculation of air over a significant portion of the rotor (black region of Figure 2). This can result in a significant loss in thrust, and a tendency to settle, even as the collective is increased. The vortex-ring region typically includes significant vibration and/or roughness.

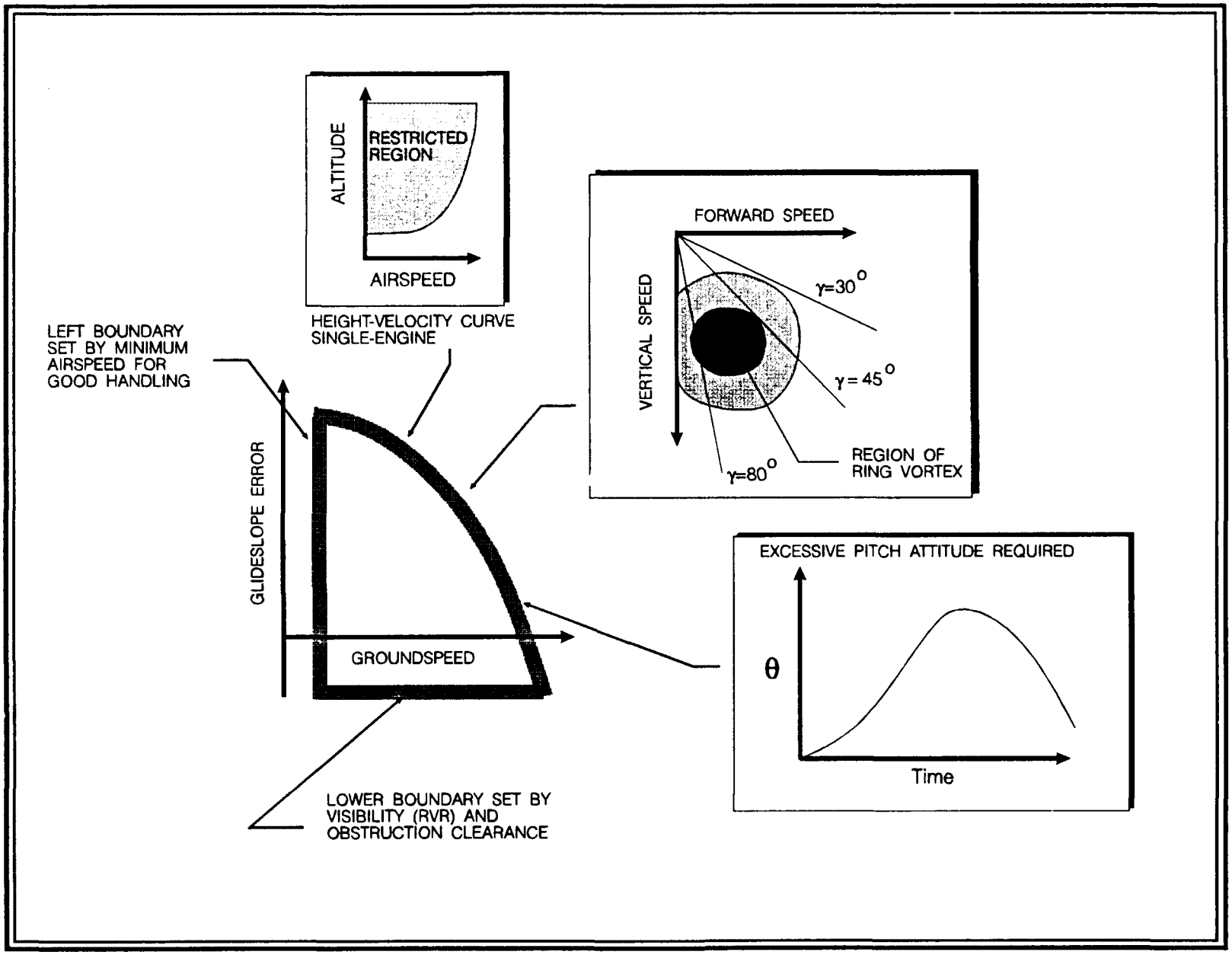

Figure 2. Basic Rotorcraft Limitations That Affect Decision-Height Boundaries

For $\gamma \leq 20^{O}$,

$$\gamma_{aero} \approx \gamma_{inertial} \left(1 + \frac{V_{wind}}{V_{airspeed}}\right)$$

where $\gamma_{Inertial}$ would be equal to γ_f to make the pad from the decision point, and a positive wind is a tailwind. Practically speaking, it is unlikely that an approach would be conducted in tailwinds strong enough to increase the aerodynamic flight path angle to values large enough to enter the vortex ring state for glideslopes of 12^{O} or less. However, for steeper glideslopes, it may become a limiting factor.

The maximum pitch attitude illustrated in Figure 2 is related to performance, in that the only way to convert low power to deceleration along the flight path is through pitch attitude. Hence, the peak pitch attitude is a measure of the power, or energy deficiency, that can be converted into deceleration without changing flight path. Because of the steepness of the constant power curves at very low airspeeds (backside of the power-required curve), simply holding collective constant while decelerating results in a rapid need for increasing pitch attitude as speed approaches zero, to hold flight path angle constant (e.g., like in a quickstop maneuver). A fast condition at breakout can result in a need for significant deceleration all the way to hover. In such cases, the pilots in the present experiment were observed to delay adding collective until the very end, and as a result, large peak pitch attitudes occurred just prior to hover. The magnitude of the peak pitch attitude is directly related to the minimum power that the pilot is willing to use in the final deceleration to hover. This is discussed in more detail in Section IV.

The left side of the decision-height window is defined by the minimum airspeed that can be comfortably flown during the transition from IMC to VMC. Many helicopters do not posses good flying qualities in the transition region from hover to effective translational lift. For example the test aircraft (a Bell 205A) tended to "buck and gallop" when operating in this region, which was considered as unacceptable by the pilots (HQR = 7). The low airspeed limit may also be set by the minimum airspeed for which IFR flight is approved. Once a minimum acceptable airspeed is established, the left boundary becomes a function of the tailwind (groundspeed = airspeed + wind) between the decision point and hover.

The lower (bottom) boundary of the DH window does not depend on the rotorcraft flight dynamics, since in the limit, the rotorcraft would fly level or even climb slightly to reach the hover point. Therefore, as noted in Figure 2, the lower limit is set by obstruction clearance and visibility constraints.

Returning to the upper boundary, it would be useful to characterize the total energy dissipation required to transition from the decision point to hover in terms of rotorcraft performance data. In that context, it is convenient to borrow a concept developed to define the vulnerability of powered lift STOL aircraft to wind shear, called the effective flight path angle, or γ_{eff} (e.g., see Ref. 5). The effective flight path angle, as it is applied to the present problem, is defined in Figure 3. This definition is an approximation which works well for glideslope angles (γ_O) of 20^{O} or less, and a more complete definition and derivation is given in Appendix B. The $V^2/2g$ term may be thought of as proportional to the kinetic energy, ($h_{DH} - h_{HOV}$) as proportional to the potential energy, and γ_{eff}/γ^{O} as a measure of the total energy that must be dissipated. This concept allows one to lump

$$a_x = \dot{V}_I + g \sin \gamma_a$$

$$g \sin \gamma_{eff} = a_x$$

$$\dot{V}_I = \frac{V_{DH}^2}{2R}$$

R = Range to Hover at DH

V_{DH} = Groundspeed at DH

$$\sin \gamma_{eff} = \frac{V_{DH}^2}{2gR} + \sin \gamma_a$$

Energy to decelerate

Angle between horizon and airspeed vector required to reach pad

IN TERMS OF GLIDESLOPE ERROR AT DH
(FOR $\gamma_o < 20^o$)

$$\frac{\gamma_{eff}}{\gamma_o} \doteq \frac{1}{(h_{DH} - d_\varepsilon)} \left(\frac{V_{DH}^2}{2g} + h_{DH} - h_{HOV} \right)$$

E.G., FOR DH = 50 FT AND A 10 FT HOVER,

$$\frac{\gamma_{eff}}{\gamma_o} = \frac{1}{50 - d_{50}} \left(\frac{V_{DH}^2}{2g} + 40 \right)$$

Figure 3. Definition of, and Approximate Equation for Effective Flight Path Angle

the deceleration requirement and geometric flight path angle into a single "effective" flight path angle. The advantage of this is that γ_{eff} can be plotted directly on the rotorcraft γ vs. V performance curves as shown in Figure 4. These example γ vs. V curves are for the XV-15 tilt rotor aircraft in the helicopter mode. In the example shown in Figure 4, the nominal glideslope angle is 12°, the groundspeed at the 50 ft decision height is 20 kts, and the rotorcraft is assumed to reach the decision height with a 25 ft glideslope error. The component of γ_{eff} due to the geometric flight path angle from the decision point to a 10 ft hover (γ_f in Figure 1) is 19.2°; 12° due to the nominal glideslope, and 7.2° due to being 25 ft high. The component of the effective flight path angle due to the need to decelerate from 20 kts to zero groundspeed is 8.5° (the V^2 term in Figure 3). This results in a total effective flight path angle of 27.7°.

The effective flight path angle will be the basis for mapping the rotorcraft performance capability on to the "decision height coordinates", defined here as glideslope error vs. groundspeed at DH (d_ϵ vs. V_{DH}), and for extrapolating the results of this program to other rotorcraft and glideslope angles.

III EXPERIMENTAL SCENARIO AND RESULTS OF INITIAL EXPLORATORY RUNS

The NRC variable stability Bell 205A was configured to have handling qualities similar to a current rotorcraft with a limited authority stability augmentation system (e.g. the Sikorsky S-76). A conventional cyclic stick and collective were provided as cockpit controllers. The initial phase of the testing was to determine the γ -V characteristics of the Bell 205A to allow estimates of the decision height window based on the effective flight path angle. The resulting γ - V curves are shown in Figure 5. It should be noted that the horizontal component of the airspeed vector is plotted as the x coordinate in Figure 5 to allow a direct comparison with groundspeed at DH (i.e. so airspeed = groundspeed in zero wind).

The nominal glideslope angle in the experiment was 9°, and some runs were made with a 6° glideslope. Initial testing indicated that glideslope angles of over 9° resulted in excessive down collective requirements for glideslope corrections in the Bell 205.

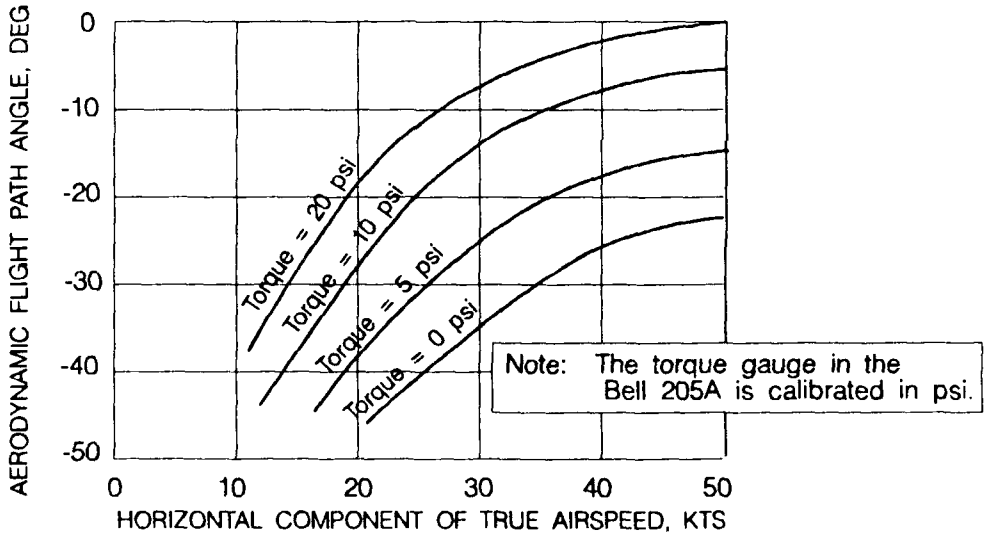

Figure 5. Flight Path Angle vs. Airspeed (γ vs. V) for the Bell 205A

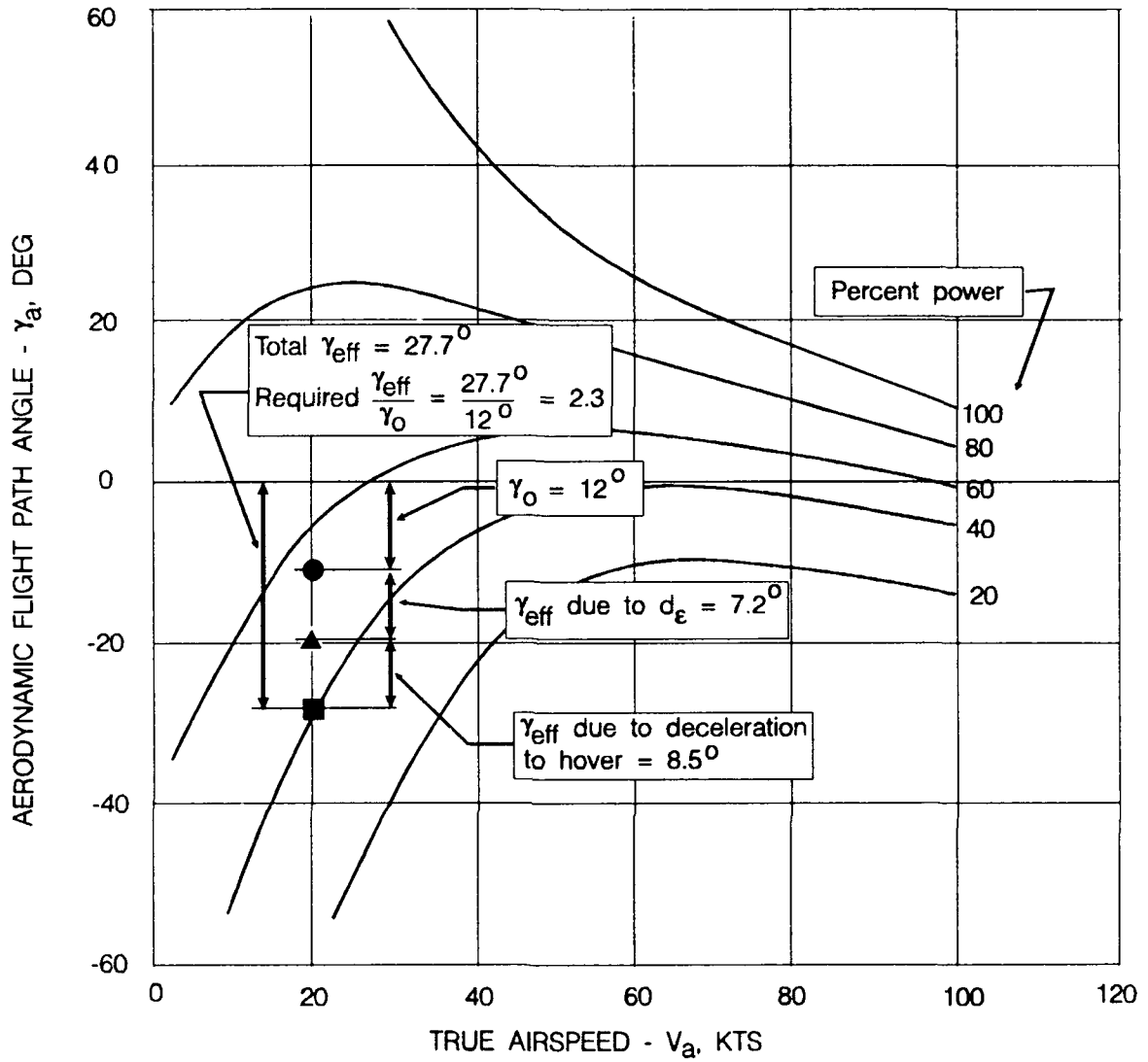

Figure 4. γ - V Curves for XV-15 Tilt Rotor Aircraft With Example Showing Components of γ_{eff}

Each run was initiated in level flight on the localizer, or just prior to turn-on to the final approach course. The evaluation pilot flew the precision approach to a 50 ft decision height in simulated instrument meteorological conditions (IMC), and completed the approach to a hover over the helipad visually (below 50 ft AGL). IMC was simulated by means of electronically fogged goggles, which were wired to the radar altimeter, and which automatically cleared at 50 ft thereby simulating breakout. The goggles were cleared on every approach so that the evaluation pilot did not have to make the missed-approach decision at DH. A series of runs was flown wherein the fogging level was set so that the evaluator could barely make out the pad at DH, and the goggles did not clear. These runs were included to look at the effects of poor visibility (i.e. scud) during the visual segment.

As noted earlier, this experiment was accomplished in the context of an exploratory study to gain an overall appreciation of the important contributors to the DH window, and to gain an appreciation of the order of magnitude of the window dimensions. Most of the experiment focused on a 9^{O} glideslope, with a breakout to clear conditions at 50 ft, where the IMC portion of the approach was flown manually using the 3-cue flight director. Other factors that were considered (mostly during initial testing) are summarized below.

- A few runs were made to investigate the effect of changing glideslope angle from 9^{O} to 6^{O}.

- A comparison was made between manual flight directed instrument approaches and fully coupled instrument approaches, in terms of the transition from IMC to VMC at DH. The manual approaches were accomplished with the 3-cue flight director utilized in a previous joint FAA/NRC study of decelerating instrument approaches. Those results are reported in an FAA report in Ref. 6, and in an NRC report in Ref. 7 (Ref. 6 is referred to in the remainder of this report for simplicity). The fully automatic approaches utilized the coupler developed in the Ref. 6 study, and a button was added to the stick to allow for autopilot disconnect at DH.

- The effect of detail on the surface of the helipad was investigated by creating two pads, each having the dimensions of 100 ft on a side. Pad A was outlined by an orange traffic cone in each corner, and one in the center, whereas pad B contained three cones on each side, a cone in the center, and cones marking the lead-in to the pad for 350 ft. Most runs were made to pad A.

- An investigation was made of the effect of a breakout to ideal visual conditions vs. fog, where breakout consisted of a dim view of the helipad through the electronically fogged goggles.

The deceleration profile was taken from the Ref. 6 work, and consisted of a constant attitude deceleration of about .045 g. from 60 kts groundspeed to a nominal 20 kts groundspeed at DH. The radar altitude box on the EADI, and the digits within the box flashed at 10 ft above decision height, and remained flashing while below this height.

Initial comparisons of runs with the 6^{O} and 9^{O} glideslope did not indicate a dramatic difference in the ability to transition from IMC at DH to hover over the pad. Therefore, most runs

were made using the steeper, and hence probably more critical, 9^{O} glideslope. The results of runs with the 6^{O} glideslope are presented and discussed in Section VI.

Nearly all of the runs were made using the manual flight director for the IMC portion of the approach. A few coupled runs were made, and these indicated that the transition was slightly more difficult because of the additional workload of disengaging the coupler, and transitioning into the control loop. There was some concern that the details of the mechanization of the autopilot cutoff could have a significant impact on the results, so it was decided to proceed with manual approaches for this initial exploratory program. An additional motivation for using the flight director was to gain more insights relative to problems encountered during the Ref. 6 program. These flight director issues are also discussed in Ref. 8.

The helipad measured 100 ft. on a side, and its perimeter was marked with three orange traffic cones on each side (a total of eight cones). Several runs were made to a modified helipad wherein additional cones were used to define two lead-in arrows which covered a distance of 350 ft. These lead-in cones were found to be of little or no value because they were under the nose almost immediately after breakout. In actual practice, such lead-in guidance would be useful to maximize the lower boundary of the DH window by extending the range of the "helipad environment". It was hypothesized by one pilot that lead-in strobes surrounding the pad, and pointing the way to the center of the pad, would be useful to assist in finding it immediately upon breakout, especially with a lateral offset.

As discussed above, an attempt was made to gain insight into the effect of poor visibility after breakout by leaving the goggles fogged at some intermediate level. These results are discussed briefly in Section IV. However, the simulation of degraded visibility was felt to be somewhat unrealistic due to a lack of appropriate graininess vs. altitude cues, and a lack of helipad lighting and visual approach aids, which would surely be present in operational use. Also, the available visibility on each run was strongly dependent on the sun angle, and cloud conditions.[4]

The effect of steady winds, windshear, and turbulence on the transition from DH to hover is known to be significant. However, setting up a tower to measure the winds at DH for each run was beyond the scope of this experiment. The winds at 500 ft AGL (before the deceleration phase) were calculated from the aircraft states for each run, but this could not be done for lower altitudes because of inaccurate airspeed measurement at lower airspeeds. In addition, the pilots attempted to keep records of the tower reported winds (which were at about 50 ft AGL) during the runs (albeit, with varying degrees of success). The effects of the estimated winds on the results are discussed in more detail in Section IV.

The majority of the runs were made to obtain estimates of the size and shape of the critical upper boundary of the decision-height window using a 9^{O} glideslope angle. The conditions at DH were systematically varied by injecting errors into the flight director control laws. The raw data displayed to the pilot was not affected so the pilot was aware of the errors at DH, as he or she would be in actual operations. This provides a valuable cue since the pilot "knows where to look" for the

---

[4] The nature of the fogged goggles is such that the visibility is essentially zero if the sun is in the pilot's eyes. The sun conditions varied from run-to-run due to a broken cloud condition on the test day.

pad during the first few critical seconds after breakout (e.g., if the raw-data localizer indicates right of course, the pad will be to the left at DH unless a large left crab angle has been established, etc., etc.). The centered flight director, with non-centered raw data is also reasonably realistic, and could represent a recovery from a large disturbance, or from a period of divided pilot attention.

Systematic variations of localizer errors were beyond the scope of the program. However, the lateral flight director was degraded from the Ref. 6 study, and this resulted in random localizer errors at breakout which ranged from zero to about 60 ft. In most cases the lateral errors were corrected by means of a constant heading sideslip to the pad, and were not considered to be objectionable.

The focus of the evaluations was on the segment from DH to hover. Each pilot was requested to provide a Cooper Harper Handling Qualities rating (see Figure 6) for that task, as well as a decision as to whether or not the transition from DH to hover would be acceptable for operational use. Time histories of the rotorcraft position, body attitudes and rates, and control positions were recorded for each run, and the wind at 500 ft AGL was automatically calculated and recorded. The value of γ_{eff} at DH (50 ft Radar altitude) was calculated and recorded for each run (using the complete expression derived in Appendix B). Glideslope error, localizer error, and groundspeed at DH were also automatically printed out. Data was collected for four pilots. Two pilots were test pilots from the NRC, one is an FAA certification pilot from the Southwest region, and the other is the author of this report. All are commercially rated helicopter pilots with significant experience in handling qualities flight testing, and the use of the Cooper Harper handling qualities rating (HQR) scale.

The use of the Cooper Harper Handling Qualities rating scale for this experiment requires some interpretation. Most of the scale applies directly except that the "aircraft characteristics" column should be interpreted as "characteristics of the transition from DH to hover". Since the handling qualities were not varied from those representative of reasonably good rotorcraft, there were no possibilities for a "loss of control", and hence, there were no ratings worse than 7 (see Figure 6). It was decided that overshooting the pad did not constitute a loss of control. The pilots were asked to make their ratings and comments following each run, while the safety pilot maneuvered the helicopter for another approach. The pilot ratings and commentary are summarized in Appendix A.

IV ANALYSIS OF RESULTS

A. Correlation of Pilot Rating Data and Commentary

A comparison of the HQRs with the acceptable-unacceptable decision (roughly equivalent to the decision to certify) in Table A-1 indicates that the dividing line is between HQR 5 and 7 where 7 is always unacceptable and 6 is sometimes acceptable and sometimes not. A correlation between the Cooper Harper Handling Qualities Rating (HQR) and the decision to certify was made in Ref. 8 for 96 separate evaluations. These results are shown in Figure 7 (taken from Ref. 8) where it can be seen that for two pilot operation, there is a 50/50 chance for certification for HQR between 5 and 6 and only an 20% chance at HQR = 7. For single pilot operation, there is a 60% chance for certification at HQR = 4, and only a 20% chance at HQR = 4.5. The single-pilot results in Figure 7 are somewhat questionable in that there was a considerable difference of opinion among the pilots, and the Ref. 6 experiment did not include realistic sidetasks to simulate single pilot workload. The boundaries and DH windows discussed below are based on the assumption of a two pilot crew i.e., all non-flying tasks were assumed to be accomplished by a co-pilot.

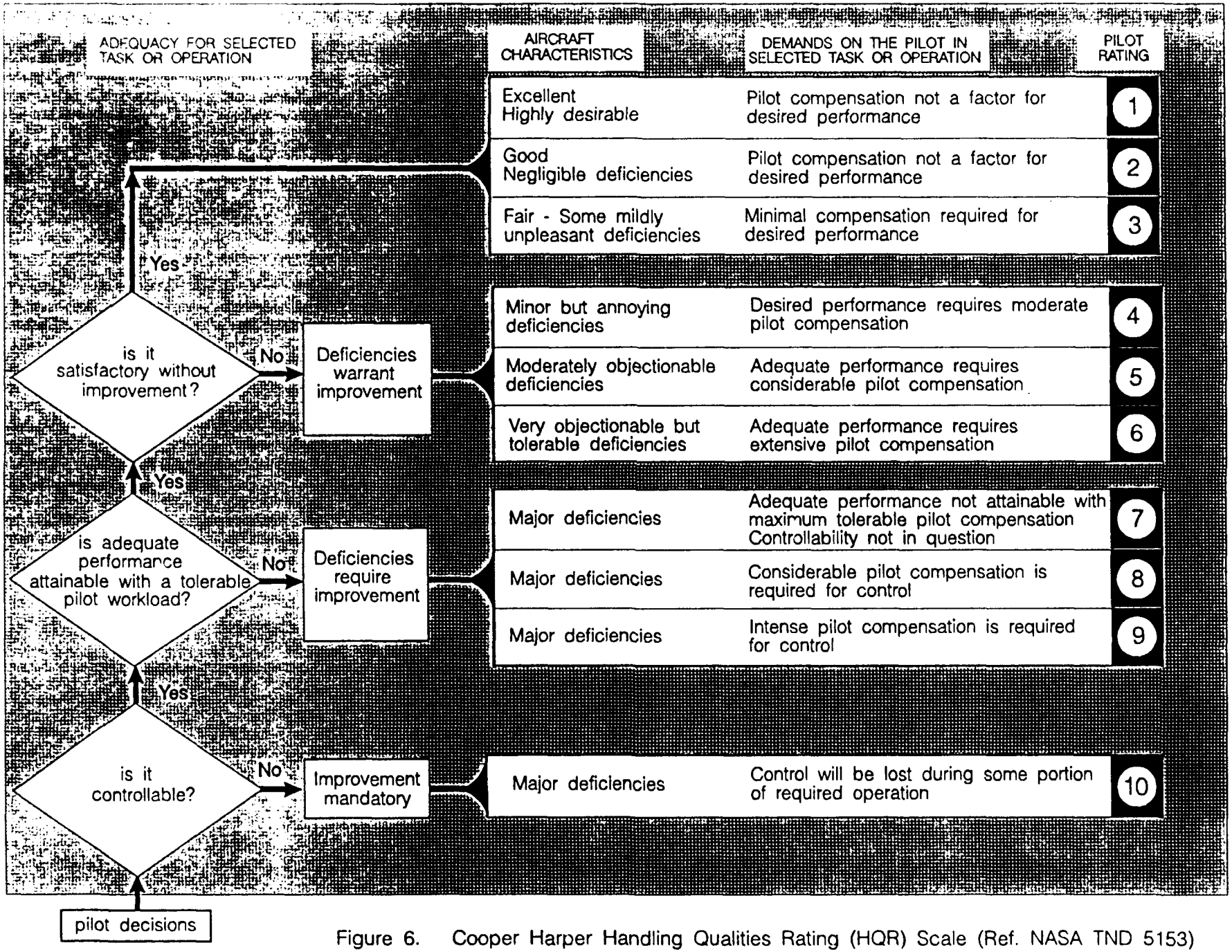

Figure 6. Cooper Harper Handling Qualities Rating (HQR) Scale (Ref. NASA TND 5153)

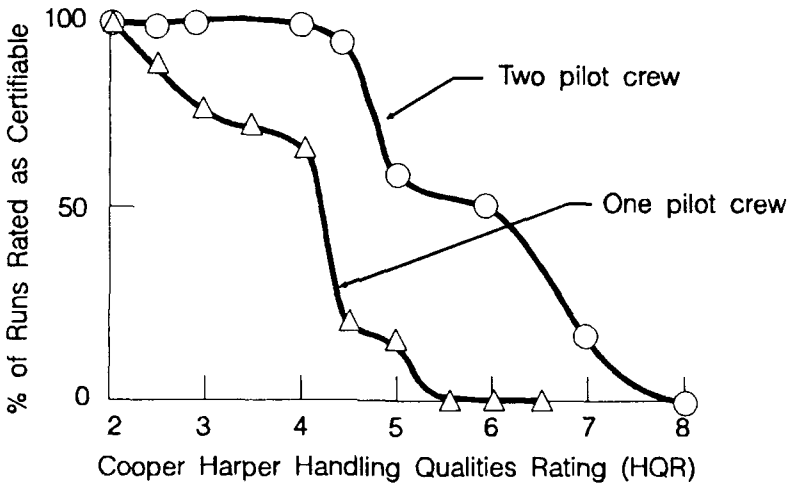

Figure 7. Decision to Certify vs. HQR From Previous Experiments

The detailed pilot rating results are presented in a spreadsheet in Appendix A along with a summary of the pilot commentary for each run. The data for the 9° glideslope and no fog after breakout are plotted on the DH window coordinates (d_ϵ vs V_{DH}) in Figure 8.

The data fairings in Figure 8 (which define the upper boundaries of several example DH windows to be discussed below) resulted from the following interpretations of the pilot rating results.

- All regions of the DH window coordinates containing points with HQR = 7 have been defined as "unacceptable", even if other data points in that region have been rated HQR = 4, and 5. The rationale is that these 7 rating(s) resulted from a slight delay or misuse of the controls in initiating the proper action from a very marginal initial condition (see pilot commentary in Appendix A). If the region is so critical that an overshoot can result from a slight delay or mistake, it should be disallowed for normal commercial operations. This interpretation of the data causes the curves to drop off steeply at speeds above 25 knots due to two points with HQR = 7 at 32 and 36 kts groundspeed (d_ϵ = -5 ft). These two data-points cause a number of cases with HQR = 4 to fall in the unacceptable region. This is discussed in more detail below.

- Regions with a large number of 6s, some 5s and an occasional 4 have been defined as unacceptable. This is based on the correlation in Figure 7, and the rationale that a Cooper Harper scale rating of 6 indicates that it requires extensive pilot compensation just to make the pad without an overshoot (i.e. "adequate performance"), and/or very objectionable but tolerable deficiencies. A region where such ratings are abundant seems excessively risky for commercial operations to very low instrument minimums. This interpretation causes the left side of the upper boundary to be flatter than it would be if only HQRs of 7 were considered as unacceptable (see Figure 8).

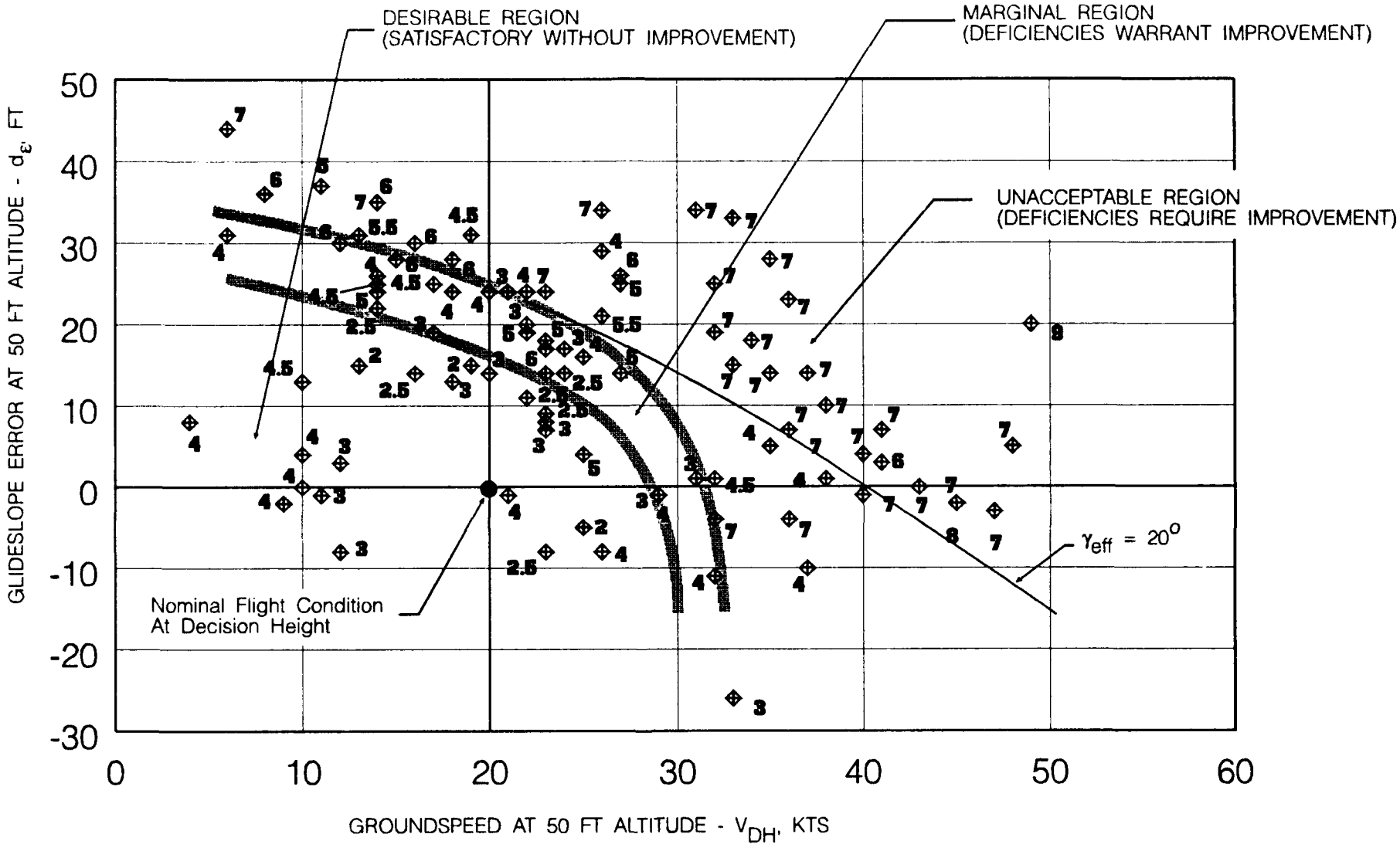

Notes: Data for 9 deg glideslope
Decision Height = 50 ft AGL

Figure 8. Pilot Ratings as a Function of Glideslope Error and Groundspeed at Decision Height ($\gamma_o = 9^o$)

- The "marginal region" contains mostly points which were assigned HQRs between 4 and 5. That is, "deficiencies warrant improvement" and adequate performance requires "moderate" to "considerable" pilot compensation on the Figure 6 HQR scale.

- The "desirable region" consists of mostly ratings of 3 or better, i.e., "satisfactory without improvement" on the Figure 6 HQR scale. A few points with HQR = 4 in this region all contain pilot comments related to vibration; a problem unique to the Bell 205A and not related to the DH window.

The desirable region in Figure 8 is proposed as a design goal for approach couplers and flight directors intended to achieve a decision-height of 50 ft following a decelerating approach in IMC conditions. The suggested demonstration would be similar to that used for fixed wing approach couplers for Category IIIa autoland systems.[5]

The outer limit of the marginal region is proposed as the missed approach boundary, and would be full scale deflection on the raw data for the final segment of the approach.

The above rationale is based, in part, on the pilot commentary for ratings which fall along and outside the faired boundaries. These are summarized on Figure 9. This figure includes the faired lines from Figure 8, and several shaded ellipses to indicate general regions of pilot commentary. The right-most ellipse indicates that the upper limit on groundspeed at DH is defined by excessive pitch attitudes and high collective activity (essentially a quickstop maneuver). Moving up and to the left, the commentary still indicates that the pitch attitude is marginally high, collective activity is excessive, and that pad visibility is becoming a problem. The left-most ellipse indicates a region where the pilots were concerned with rotorcraft performance limits associated with steep approaches, and that pad visibility has become a significant problem. It should be noted that the glare-shield on the Bell 205 is reasonably low, and that the visibility over the nose of some more modern helicopters is somewhat worse. The urgency along the upper boundary is generally classified as moderate; not a good situation for a transition from IMC to a VMC hover, at altitudes below 50 ft AGI .

The faired boundaries from Figure 8 are presented without pilot ratings or commentary in Figure 10. The shaded region on the right side of Figure 10 contains primarily HQRs of 4 to 4.5 with two notable exceptions - a pair of 7s. The upper limit of this region is defined by a line of constant γ_{eff} (γ_{eff} was defined in Figure 3). In fact, if it were not for the two pilot ratings of 7, the line of $\gamma_{eff} = 20^{o}$ would nicely separate the HQR 6 and 7 ratings from the HQR 4 and 5 ratings. Hence, it can be argued that an effective flight path angle of 20^{o} represents the limit of the energy dissipation capability of the Bell 205, as long as the pilot responds immediately, and with the correct control inputs at DH. However, if the pilot encountered some delay (such as in making a transition from fully coupled to manual flight, or lacking good speed and sink-rate cues at DH), an overshoot of the pad, and/or excessive pitch attitudes tended to result. A margin or pad is required from the

---

[5] Current fixed-wing category IIIa couplers are usually designed and certified within the guidelines of Advisory Circular 20-57A which specifies touchdown performance limits which must be achieved. Furthermore, it indicates that "a suitable computer analysis should show that under realistic environmental conditions including the wind model described in an Appendix, the touchdown performance will be such that landing outside of the prescribed dispersion area will be improbable" (i.e. probability between 10^{-5} and 10^{-9} per hour of flight).

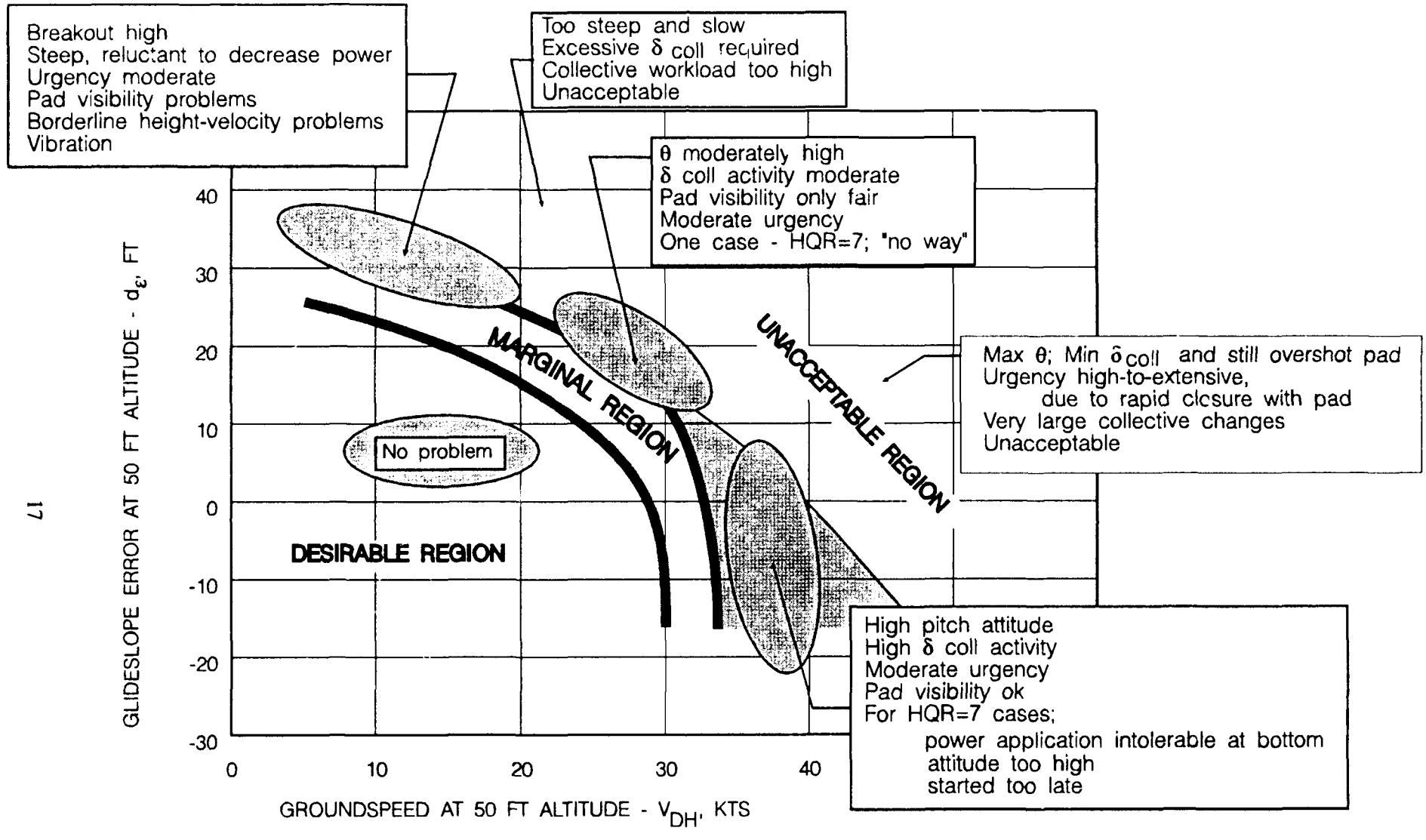

Figure 9. Summary of Pilot Commentary

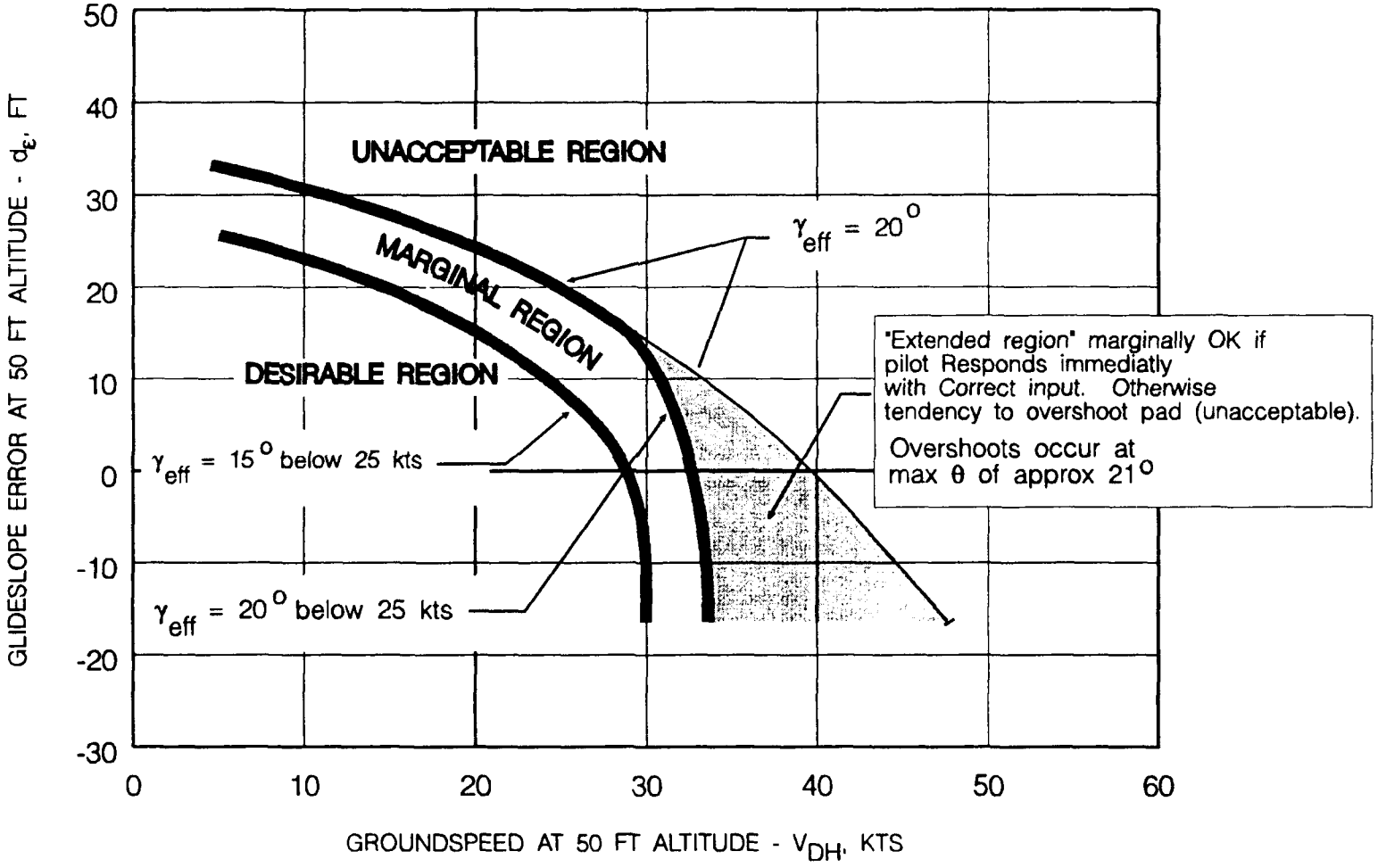

Figure 10. Extended Region for Decision Height Window

$\gamma_{eff} = 20^{o}$ line for groundspeeds above about 25 kts to eliminate the shaded region in Figure 10. A review of the time histories of runs along this more restricted boundary indicate that it results in a maximum pitch attitude of about 14^{o}. For the two runs in the shaded region where the pilots started late and assigned ratings of 7, a maximum pitch attitude of 21^{o} was observed. In fact, this is approximately the maximum pitch attitude observed for all runs in the unacceptable region for all of the pilots.

The peak pitch attitude used during the final portion of the deceleration to hover is closely correlated to the minimum power (collective position) used by the pilot. The reason for this is that the required power increases rapidly as the airspeed approaches zero. Some example collective trajectories are sketched on the Bell 205A γ - V curves in Figure 11 to illustrate the general trends noted from the approach time histories. The thick line between points A and B indicate that the pilot is holding collective constant between breakout at 35 kts and approximately 11 kts. The initial power deficiency (at DH) is due to the deceleration on the glideslope. By holding collective constant, this deficiency in power increases rapidly as the airspeed bleeds off. The only way to hold flight path angle constant, or to reduce it approaching hover with such a power deficiency, is to produce lift via increasing angle-of-attack and hence pitch attitude (recall $\theta = \alpha + \gamma$). This higher angle-of-attack causes the drag to rise sharply, producing the necessary deceleration to recover from a fast condition at decision-height. At point B, the airspeed is too low to produce significant lift ($L \propto 1/2\rho V_a^2$), and the power deficiency must be eliminated by rapidly increasing power to that required for hover (i.e., between points B and C on Figure 11). From this discussion it can be seen that the peak pitch attitude is directly related to the power deficiency, and therefore the constant torque line (e.g., between points A and B in Figure 11). It is therefore not surprising that the steep upper boundaries which correlate the pilot rating data in Figure 8 are well fitted by lines of constant torque (power). This is illustrated in Figure 12 where it can be seen that the data fairings (thick lines) follow lines of constant torque after departing lines of constant γ_{eff}. The usefulness of this observation will be discussed in more detail in the formulation of example decision-height windows (DH windows) in Section V.

A review of the pilot commentary indicated that the primary deficiencies that resulted in degraded pilot ratings (say, HQR $\geq$ 5) were directly associated with the factors discussed above, i.e., excessive pitch attitude, and excessive collective activity. Analysis of the time histories revealed that the pilots pitch attitude and collective control strategies were very similar, and can be characterized as discussed below and by the time histories in Figure 13.

- The pilots very rarely decreased collective pitch, and never decreased the power by a significant amount after reaching decision height (as described by the constant torque line between points A and B in Figure 11).

- For cases where the helicopter was essentially on glideslope and speed at DH (e.g. Figure 13a), the change in collective pitch and pitch attitude from breakout to hover was characterized by a gradual ramp and a pitch attitude change of only about 2 to 3 degrees. The small pitch attitude requirement is a direct consequence of the increased power (and hence small power deficiency) as the helicopter slows to speeds well on the backside of the power required curve. Pilot commentary for this run: "no problem - HQR = 3". The collective activity for this run would be well approximated by the thick line between points D and C in Figure 11.

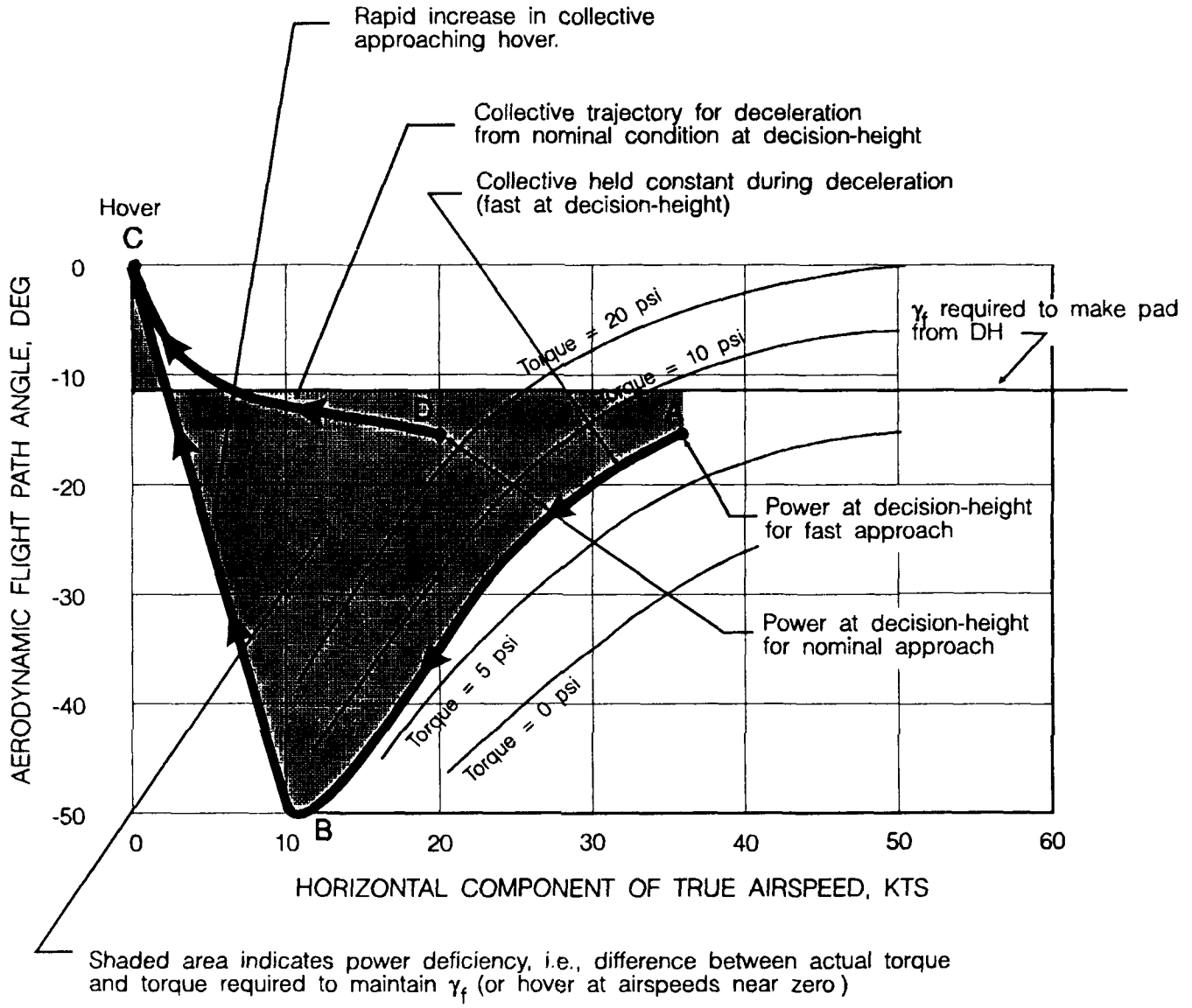

Notes:

1. A - B - C is collective trajectory for fast condition at DH
2. D - C is collective trajectory for nominal condition at DH
3. Both examples have same γ_f at DH

Figure 11. Characteristics of Collective (Torque or Power) as a Function of Deceleration Requirement From Decision-Height to Hover

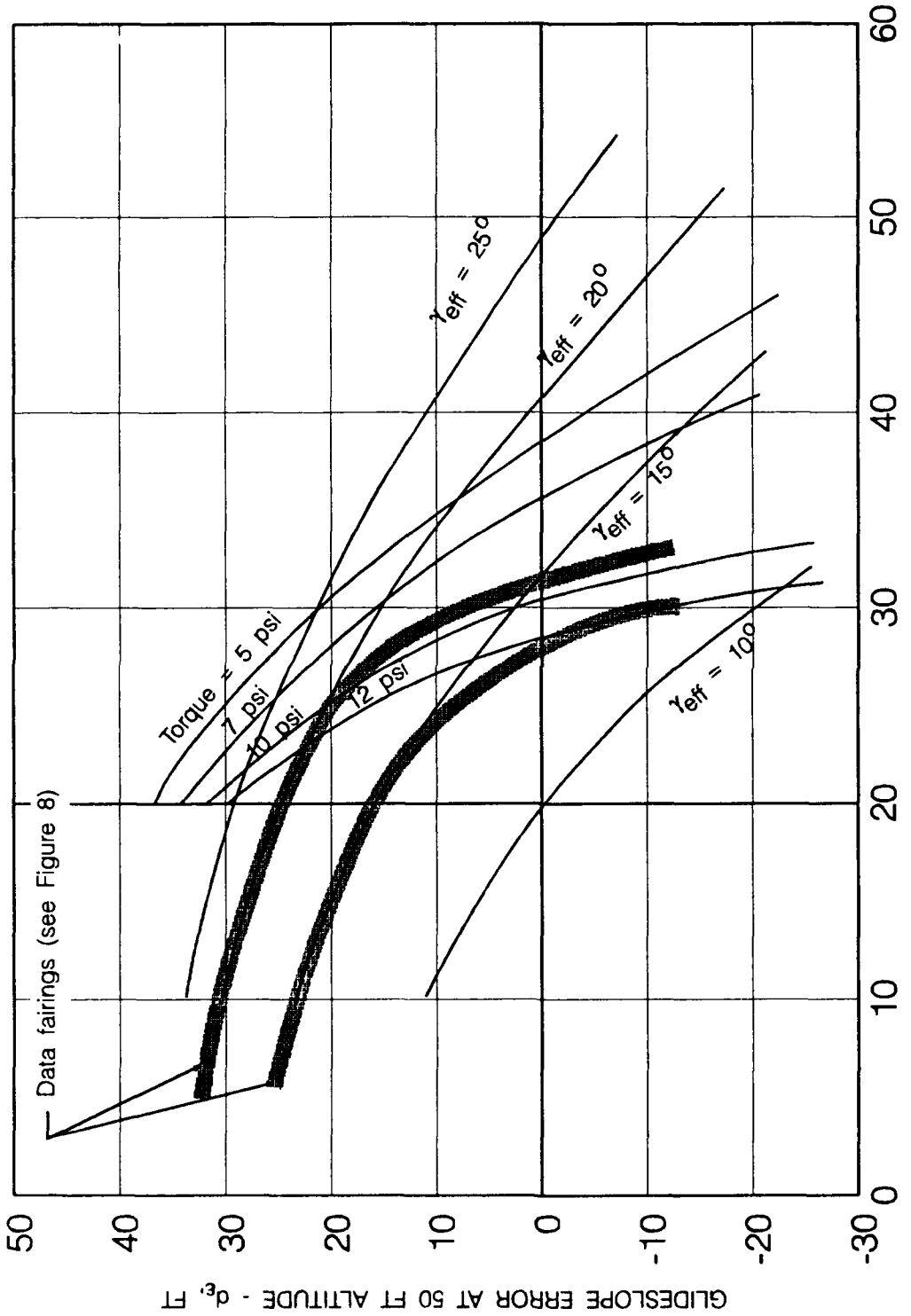

Figure 12. Lines of Constant γ_{eff}, and Constant Torque Plotted on Decision Height Window Coordinates ($\gamma_o = 9^o$)

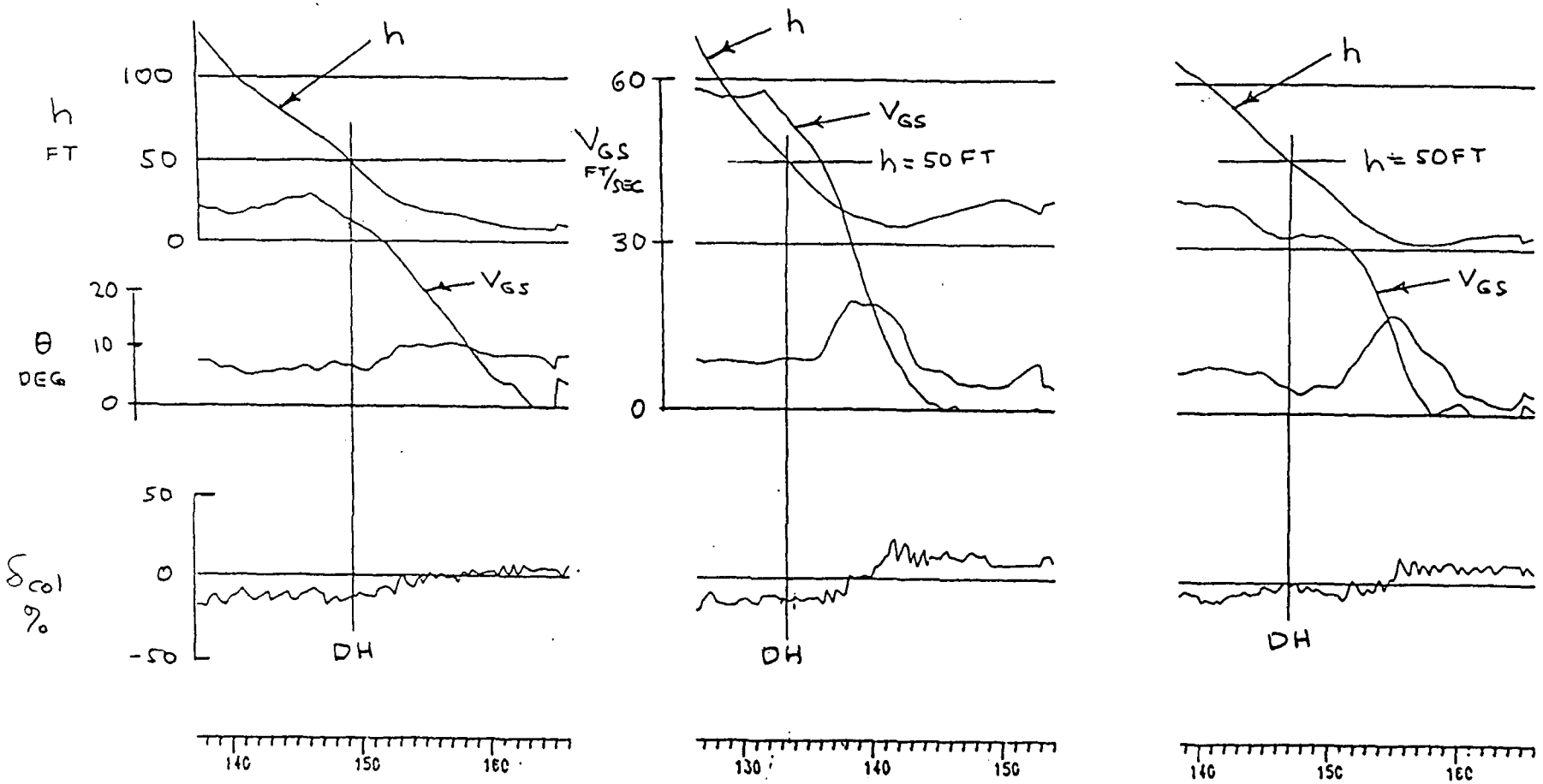

a) Nominal Approach

d_ε = 7 ft.
V_{DH} = 22 kts.
γ_{eff} = 12.7°
HQR = 3

b) Fast Approach

d_ε = 7 ft.
V_{DH} = 33 kts.
γ_{eff} = 17.9°
HQR = 6

c) High Approach

d_ε = 18 ft.
V_{DH} = 21 kts.
γ_{eff} = 16.2°
HQR = 5.5

Figure 13. Example Time Histories From Decision-Height to Hover

- For cases where the helicopter was fast at DH (e.g., Figure 13b), the pilots held collective pitch essentially constant after breakout, and increased pitch attitude as required to maintain the visual glideslope to the pad. As the rotorcraft slowed to speeds well on the backside, the required pitch attitude rapidly increased (e.g. see Figure 13b and c) due, in part, to the need to arrest sink, but mostly to the rapidly increasing power deficiency at low airspeeds as discussed above. All of the collective required for an in-ground-effect (IGE) hover was abruptly added as the groundspeed approached zero (about 5 kts), and the nose was lowered to achieve the hover attitude just as the groundspeed reached zero. The pilot commentary for the run shown in Figure 13b were: "Unacceptable - a lot of collective required to assist in breaking, and to keep altitude under control, pitch attitude was extreme - urgency was very high - came to hover over pad, but downrange of center - HQR = 6".

- For cases where the helicopter was high at DH (e.g., Figure 13c), the pilots either decreased collective a very small amount, or held it essentially constant, and pitched down 3 or 4 degrees followed by an abrupt pitch-up maneuver at the end (as required to arrest the sink rate without adding power). The collective was added abruptly at the very end to achieve the IGE hover. Pilot commentary for the run in Figure 13c: "Required pitch attitude and collective moderately high - moderate sense of urgency - borderline acceptable - came to hover slightly downrange of center of pad - HQR = 5.5".

- Comments related to " a lot of collective activity" often refer to the fact that all of the collective was added at the very end. For example, the magnitude of the collective change from decision height to hover is essentially the same for the runs in Figure 13a and 13c., but the commentary and ratings reflect that the collective "activity" was much higher for 13c.[6]

The time histories in Figure 13 are representative, but as might be expected, each run exhibits some variation from these shapes. The deceleration from DH to hover is seen to be anything but constant, and varies from run to run according to the attitude and collective motions. For this reason, it would be hopeless to attempt to characterize these time histories to define decision height window boundaries. The approach to resolving this dilemma in the present program has been to utilize the concept of an effective flight path angle which is proportional to the total energy that must be dissipated between DH and hover.

B. Effect of Wind

A detailed investigation of the effect of wind on the decision-height window was beyond the scope of this exploratory program. The primary problem of isolating such effects in full scale testing has to do with the identification of the actual wind and windshear between DH and hover. Such

---

[6] The absolute value of collective position cannot be obtained from the time histories since it depends where the evaluation pilot set the controller when the variable stability system was engaged. This tended to vary from run to run. However, the magnitude of the collective changes in Figure 10 can be estimated by noting that full travel is 10.7 inches. Hence the collective changes in Figure 10 vary from approximately 1.5 to 3 inches.

measurements would require a 50 ft anemometer tower near the DH point, and a second anemometer at the hover point as a minimum. An alternative approach would be to identify the wind from the rotorcraft states. However, this would require accurate measurement of airspeed between DH and hover, and such measurements were not possible with the available instrumentation. An estimate of the wind conditions during the tests was obtained by using the aircraft states to measure the wind at 500 ft AGL (where the airspeed measurement was still accurate as the airspeed was on the order of 60 kts). A second estimate was made by noting, and recording, the winds reported by the Ottawa control tower. This resulted in a reasonable estimate since the test site was on the Ottawa International airport, and the tower anemometer is located at an altitude of about 50 ft AGL.

The wind values from the measurement at 500 ft tended to be somewhat higher than the winds reported by the tower, so the tower winds were used in the present analysis as more representative of the conditions at the 50 ft decision height. The headwind and tailwind components of these winds were calculated and tabulated in the data summary in Table A-1 (Appendix A). The effective flight path angle has been calculated and tabulated in this table both for a no-wind condition, and for the estimated wind at DH. The pilot rating data for each run with a 9^{o} glideslope are plotted on the DH window coordinates with symbols which are representative of the wind estimates for that particular run on Figure 14. The pilot ratings for the tailwind cases are circled to assist in identifying those cases. It was expected that the tailwind cases would be downrated compared to a no-wind or headwind case, because the aerodynamic flight path angle is increased in tailwinds, i.e., $\gamma_{aero} = \gamma_{inertial}\,(1 + V_{wind}/V_{airspeed})$ where a tailwind is positive. The physical phenomenon expressed by this equation is quite noticeable on an approach in a tailwind where significantly less power is required to maintain glideslope than for a no-wind or headwind condition. The equations in Appendix B indicate that the effective flight path angle is affected by the wind (as it should be, since it is directly associated with the aerodynamic flight path angle), and this is reflected by the numerical values for the no-wind γ_{eff} (NWGAMAEFF) and the γ_{eff} (GAMAEFF) columns in Table A-1.

A review of the pilot rating data in Figure 14 does not confirm, or necessarily disconfirm, the expected effect of wind. For example, it would be expected that for a tailwind, the pilot rating for a given d_{ϵ} and V_{DH}, would be worse than for a no-wind or headwind case, since the γ_{eff} (and corresponding γ_a) would have a larger negative value.[7] Unfortunately, there were no cases where a significant tailwind (i.e., a tailwind over 5 kts) existed for a case in the region of normally good pilot ratings. Nearly all of the high tailwind cases (X symbol in Figure 14) resulted in large positive glideslope errors or excessive groundspeed at DH, which could have been a result of glideslope and groundspeed tracking problems in a tailwind, or could have been a quirk of the experimental protocol (i.e., most of the runs in a significant tailwind may have been programmed to be high and or fast). A few cases with tailwinds of 5 kts or less (triangles) did occur in the desirable region, and these do

[7] An interesting (albeit, detailed) observation is that γ_{eff} would not be expected to be a good correlator of pilot ratings. This is because larger (more negative) values of γ_{eff} (and corresponding γ_a) are not bad from the standpoint of handling qualities until a "bad region" of the γ - V plot is encountered. However, γ_{eff} would be expected to provide a hard limit beyond which the ratings will be poor (e.g. 20^{o} in this experiment, see Figure 8). For this reason plots of HQR vs. γ_{eff} are not presented.

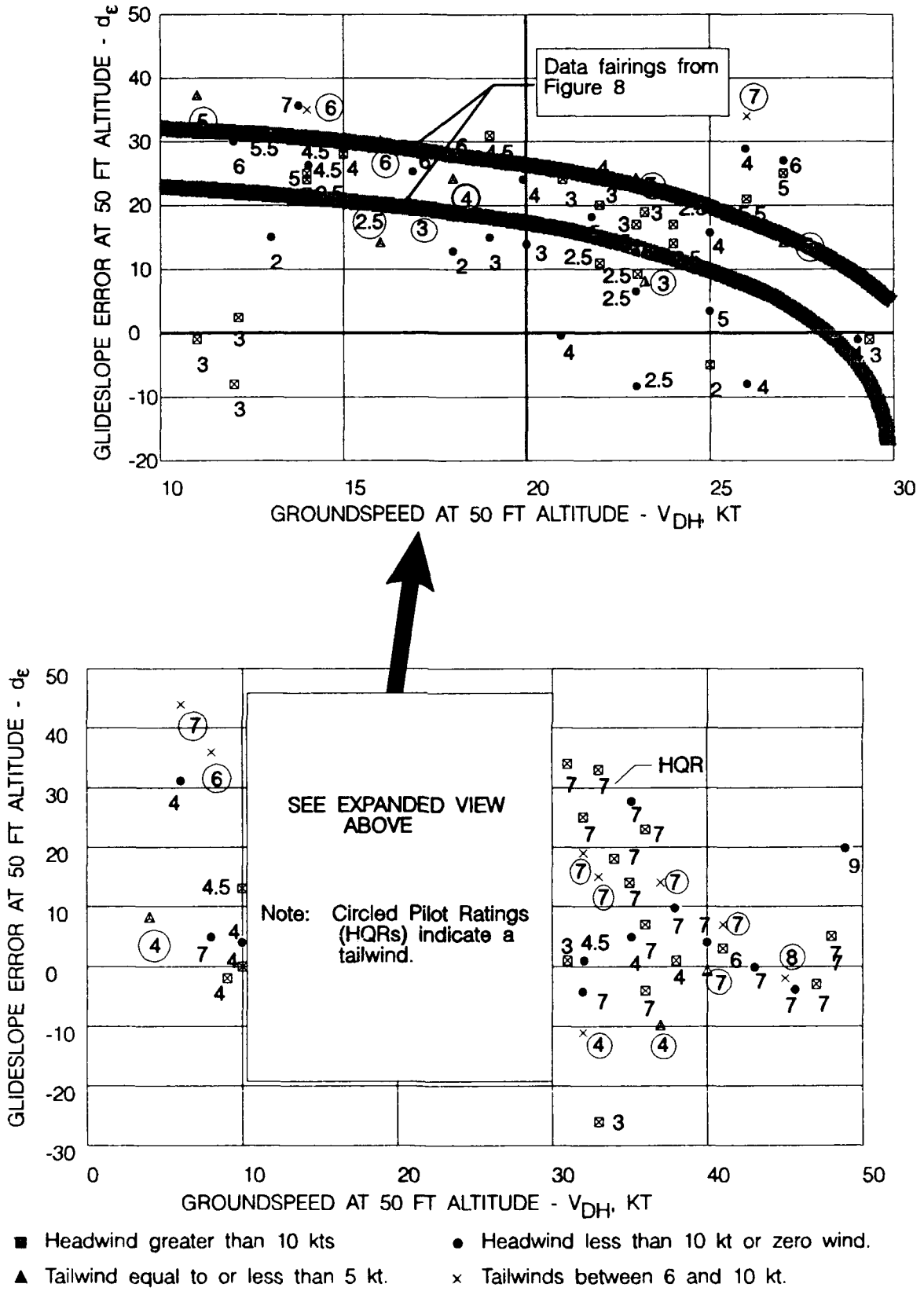

FIGURE 14. Effect of Wind on Handling Qualities Ratings (HQRs)

not indicate any differences from the no-wind or headwind cases; probably indicating that they did not result in a large enough change in γ_{eff} to get into a "bad region" of the γ - V curve. It is notable that the only HQR = 7 case along the upper boundary below 30 kts was for a slight tailwind, but there is insufficient data to draw any general conclusions related to the effects of wind. This is especially true in view of the lack of precise information related to the actual winds between decision height and hover.

A systematic variation of winds and windshear would be more effectively accomplished on a ground-based simulator. It is important that the ground-based simulator have a wide field-of-view to insure that the cuing environment is similar to flight.

V. DEVELOPMENT OF EXAMPLE DECISION-HEIGHT WINDOWS

It is not within the charter of this research to specify a decision-height window. The example DH window definitions presented in this section are intended to convey insights and rationale obtained from the conduct of the experiment and analysis of the results.

A. Factors Which Define the Left Boundary of the DH Window

As noted in Figure 2, the left boundary of the DH window is defined by the low airspeed limit of the rotorcraft. Excessively low airspeed at DH can be a function of one or more of the following factors.

- Degraded handling qualities. Rotorcraft handling qualities tend to degrade with decreasing airspeed for two reasons; 1) dynamic modes become less stable or unstable and, 2) operation in the transition region between hover and forward flight can result in severe vibrations and/or uncommanded "bucking and pitching motions". If the augmentation system gains are not tailored to account for these effects, the handling qualities will be unacceptable for IMC and the transition from IMC to VMC.

- Flight in the restricted height-velocity envelope. This usually applies only to single-engine rotorcraft. However, if the altitude loss following an engine failure near DH is significant (a few feet is significant at 50 ft in IMC conditions), some restrictions will apply.

- It is possible to inadvertently enter rearward flight. This phenomenon has been observed on numerous occasions for low speed instrument flight in military over-water operations. Inadvertent rearward flight usually results in complete loss of control. Unless the flight control system can protect against such an occurrence, a reasonably healthy margin is necessary, along with some method of alerting the pilot to an excessively low airspeed condition.

Since the left boundary of the DH window is defined by airspeed, and the right boundary by groundspeed, the dimension of the window will vary with the ambient wind between DH and hover. For example, if the DH window is defined by a low airspeed limit of 10 kts, and an upper groundspeed limit of 30 kts, the speed dimension of the window is $\pm$ 10 kts for a nominal groundspeed of 20 kts at DH. However, if a 10 kt tailwind exists at

DH, the groundspeed dimensions of the DH window become 20 kts and 30 kts. For a nominal 20 kt groundspeed, the tolerance of the DH window becomes -0 kts and + 10 kts.

The left boundary of the example DH windows in this section have all been set a 10 kts for illustration. This value seemed reasonable based on the flight test data.

Work needs to be accomplished to develop criteria and supporting data for guidance as to what constitutes an acceptable low airspeed limit.

B. Setting the Lower (Bottom) Boundary of the DH Window

As discussed earlier, the lower boundary is not dependent on rotorcraft performance or flying qualities. It is obviously highly sensitive to obstructions below the nominal glideslope, and to the range at which the helipad is visible from decision height (e.g., see Figure 1).

A lower boundary has not been defined for the example decision-height windows defined in this section since obstruction clearance factors were not considered.

C. Development of the Upper and Right DH Window Boundary From Rotorcraft Performance Data

The methodology for utilizing the effective flight path angle concept to develop decision-height windows from basic rotorcraft performance data is developed in this sub-section.

The physical significance of γ_{eff} is that it represents an equivalent task that is more easily understood and interpreted than the complex deceleration to hover from breakout. The "equivalent task" is to fly at a constant flight path angle ($\gamma = \gamma_{eff}$) and at the speed at DH. For example, if the helicopter arrives at the decision-height 35 ft above a nominal 9^o glideslope, and at a groundspeed of 25 kts, γ_{eff}/γ_o is calculated to be 3 (see Appendix B, or the approximation in Figure 3). Therefore, $\gamma_{eff} = 27^o$ (3×9^o), and the task of decelerating to hover is equivalent to flying at a constant speed of 25 kts and a flight path angle of 27^o. Plotting this on the γ - V curves for the Bell 205 (Figure 5), indicates that it would require a very low amount of torque (approximately 7 psi), and hence is near a basic rotorcraft performance limit.

While the γ - V curves represent the theoretical performance capability of the rotorcraft, it is well known that there are other restrictions which must be superimposed on these curves. Some restrictions are performance related (e.g., vortex-ring state, height-velocity curve, and vibration), and other restrictions tend to be centered about degraded handling qualities. The results discussed in Section IV indicated that below about 25 kts groundspeed, the limit consists of a line of constant effective flight path angle, γ_{eff}. Above 25 kts, the boundaries departed from a constant γ_{eff} by bending down sharply and thereby limiting the maximum groundspeed (e.g., see Figures 8 or 10). Interestingly these departures from constant γ_{eff} are well approximated by lines of constant torque or power. This is illustrated in Figure 12, where lines of constant torque, and lines of constant aerodynamic flight path angle have been mapped from the γ - V coordinates onto the DH window grid

of glideslope error vs. groundspeed. This mapping was accomplished by:

- interpreting γ_a as an effective flight path angle, γ_{eff}, which includes the actual geometric flight path angle and the deceleration requirements to transition from DH to hover.

- using the approximate equation for γ_{eff} in Figure 3 to obtain lines of constant effective flight path angle as a function of groundspeed and glideslope error. A hover height of 10 ft was assumed.[8]

- selecting points along lines of constant torque from the γ - V plot in Figure 5, setting γ_a equal to γ_{eff}, and noting the speed (V_{DH}) for each point. These two values (γ_{eff}, and speed) were used in the γ_{eff} equation to solve for the glideslope error, d_ϵ corresponding to each selected γ - V point. That is, from Figure 3:

$$d_\epsilon \approx 50 - \frac{\gamma_o}{\gamma_{eff}} \left(\frac{V_{DH}^2}{2g} + 40\right)$$

From Figure 12, it can be seen that the data fairings in Figures 8 and 10 can be well approximated by lines of constant effective flight path angle and lines of constant torque as follows.[9]

Nominal missed approach boundary

$V < 25$ kts -- $\gamma_{eff} = 20^o$

$V \geq 25$ kts -- Torque = 10 psi

Nominal flight director and approach coupler requirements boundary

$V < 25$ kts -- $\gamma_{eff} = 15^o$

$V \geq 25$ kts -- Torque = 12 psi

The above missed approach boundary definitions are superimposed on the Bell 205A γ - V curves in Figure 15a. Any point in the shaded area of this plot represents a flight path angle-airspeed combination that is safely flyable. It follows that once a similar shaded region for any rotorcraft is defined, its boundaries can be mapped onto coordinates of d_ϵ vs. V_{DH} (via the equation for d_ϵ noted above) to obtain a decision-height window. An example of such mapping is illustrated in Figure 15b for the Bell 205, and a 9^o glideslope angle. A

---

[8] The more exact equation in Appendix B could also be used, but the error is within 5% (and usually significantly less) for the values of glideslope angle and glideslope error that occurred in this experiment.

[9] Recall that the upper data fairing in Figure 7 (i.e., the "marginal region") has been interpreted as a missed approach boundary, and the lower data fairing (i.e., the "desirable region") as a requirement for flight director and approach coupler performance.

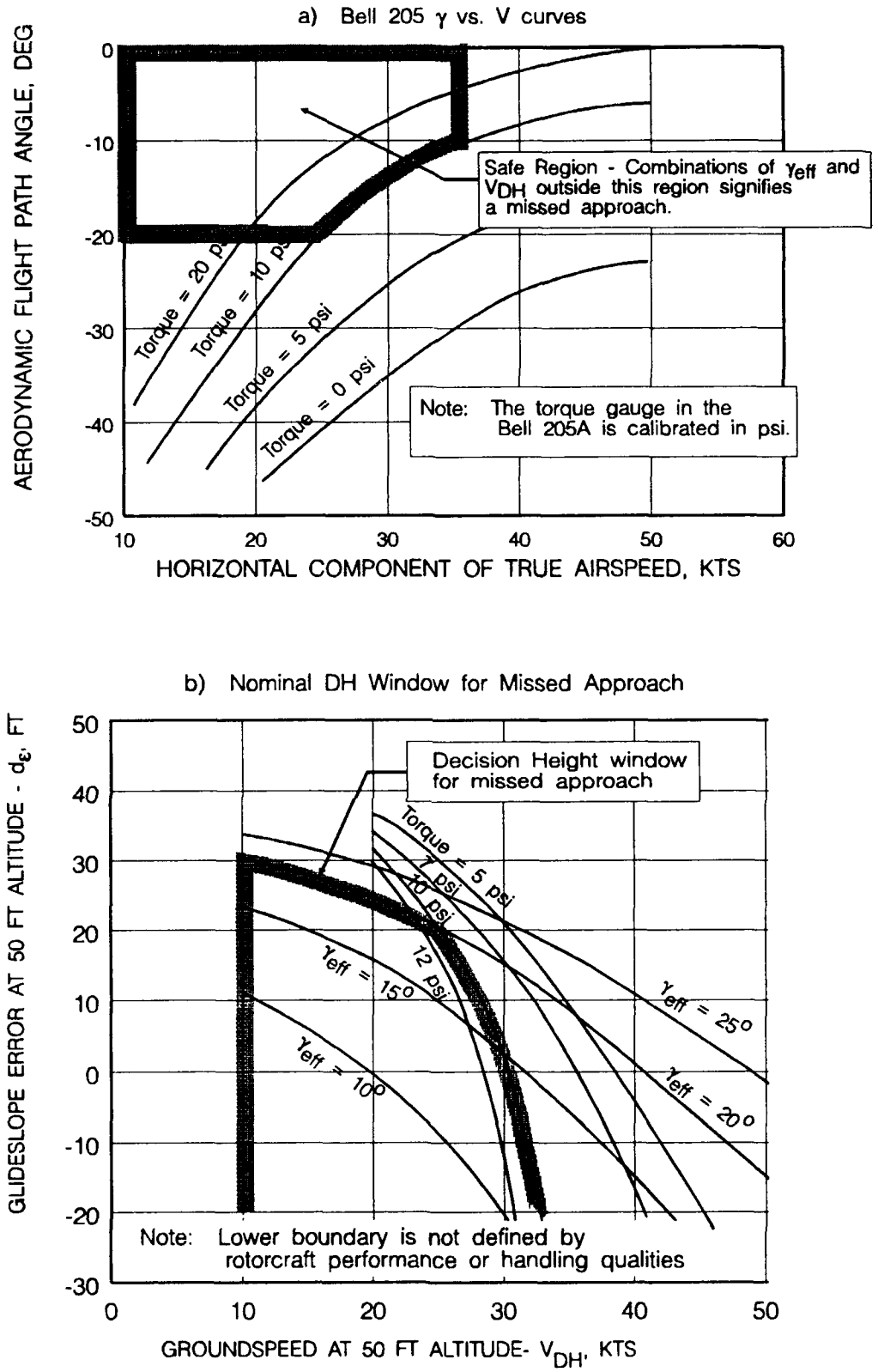

Figure 15. Bell 205A Performance Limits Mapped onto d_ε vs V_{DH} to Obtain DH Window for Missed Approach ($\gamma_o = 9^o$)

similar procedure has been carried out to illustrate the more conservative flight director and approach coupler requirements window in Figure 16. The dimensions of this window are stringent, but are reasonable in the context of the flight director and approach coupler experiments reported in Refs. 6 and 7. As discussed in Ref. 6 and in Ref. 8, the tracking results of the Ref. 6 and 7 tests were such that a fully coupled approach could easily meet the requirements of the Figure 16b DH window. However, the vertical axis flight director data indicated that glideslope errors of 25 ft were common, and therefore improvements would be required before manual approaches could be allowed to a 50 ft decision height (based on the DH window in Figure 16b).

A less conservative "extended boundary" for the missed approach window is defined if the shaded region on the right side of Figure 10 is ignored (see discussion in Section IV). This extended boundary would be defined by $\gamma_{eff} = 20^{O}$, and for reasons to be shown subsequently, by a line of constant torque of 5 psi above 25 kts. These limits are plotted on the Bell 205 γ - V curves in Figure 17a, and are mapped onto the d_{ϵ} vs. V_{DH} coordinates in Figure 17b. A comparison of the extended missed-approach window with the "nominal" window in Figure 15b indicates that the primary difference is that significantly higher airspeeds are allowed. The rationale for the less conservative extended window would be based on significantly improved cues due to helipad markings and lighting, and possibly a larger landing area or overrun. The helipad in this experiment was 100 ft on a side as compared to the pad used in the FAA tests at Atlantic City (Ref. 1) which was 150 ft on a side

As noted above, the extended DH window results from inclusion of most of the shaded region in Figure 10, and hence the two HQR = 7 ratings at V_{DH} = 32 and 36 kts. As discussed earlier, these ratings both represent cases where the pilots noted some confusion between breakout and initiating action to decelerate to hover (see pilot comments in Appendix A for cases 5 and 78). All other ratings in this region are HQR = 4 to 4.5. It could be argued that with better cuing or a larger landing area, any delays or initial misapplication of controls would be eliminated. The physical significance of eliminating the margin afforded by the "shaded region" in Figure 10 can be illustrated on the γ - V curves in Figure 17a. The upper torque limit (10 psi) represents the nominal missed-approach window, and the lower torque limit (5 psi) represents the extended missed-approach window. Consider now the following example. If the pilot arrives at DH at point A (Figure 17a), and experiences some delay in initiating the proper action at breakout (due to poor cues, etc.), it will be necessary to operate in the "extended" region (e.g., point B) to stop at the pad. That is, since the deceleration was started late, a lower torque is required to make it. The pilot rating data indicate that this is not a problem since most HQRs in the "extended region" (i.e., the shaded region of Figure 10) are 4. If, on the other hand, the extended missed approach window is used, and the pilot arrives at DH at point B and encounters the same delay (like the two 7s at 32 and 36 kts), the possibility of "making it" is very poor since he will be operating in a region of solid 7s, i.e., point C.[10] This is potentially hazardous since

[10] Point C cannot be mapped on to the DH window coordinates because the effective decision height is actually lower than 50 ft as a result of the pilot delay. However, operating at point C requires the deceleration characteristics that were found to be unacceptable in the experiments (i.e. torque < 5 psi and $\gamma_{eff} > 20^{O}$).

a) Bell 205 γ vs. V curves

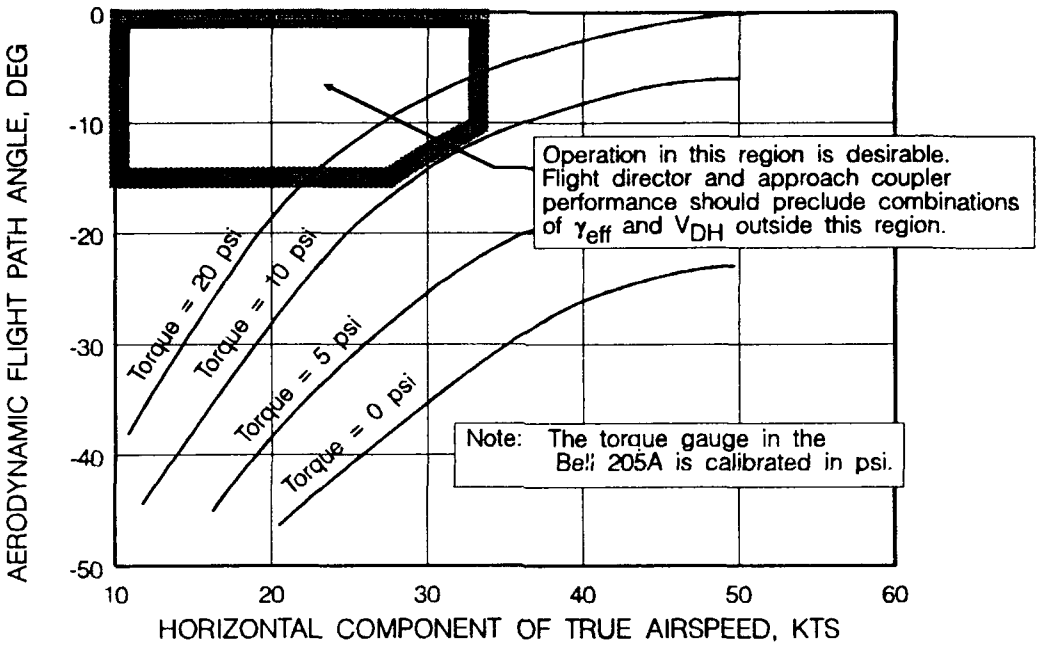

b) Nominal DH Window for Flight Director and Approach Coupler Requirements

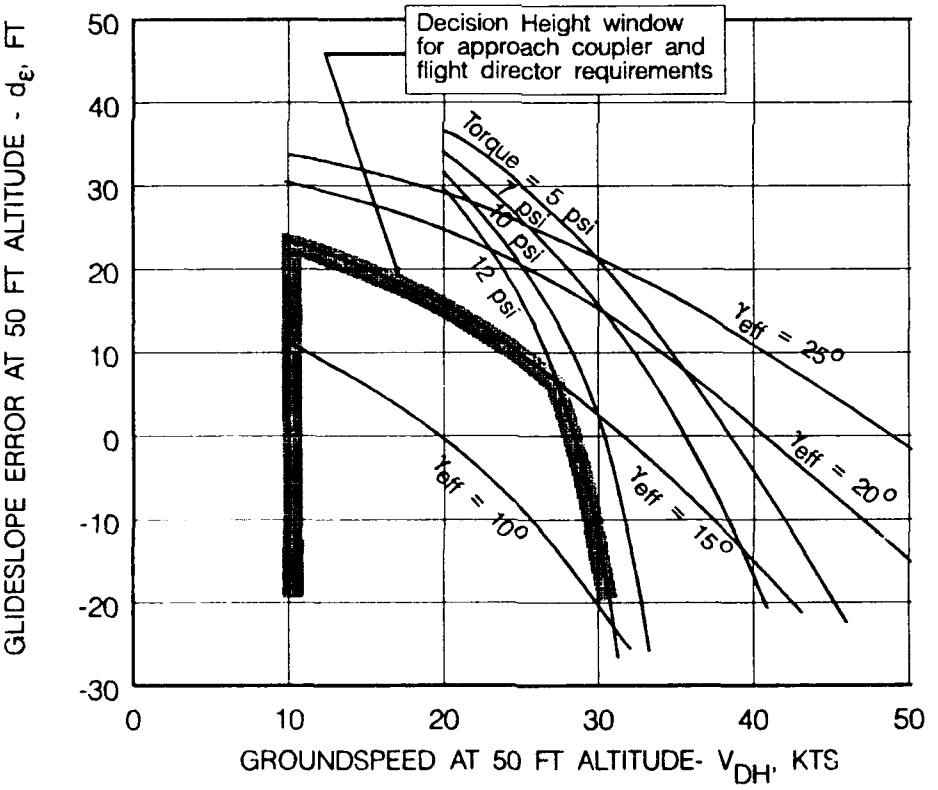

Figure 16. Helicoter Performance Limits Mapped onto d_ε vs V_{DH} to Obtain DH Window for Flight Director and Approach Coupler Requirements (γ_o = 9°).

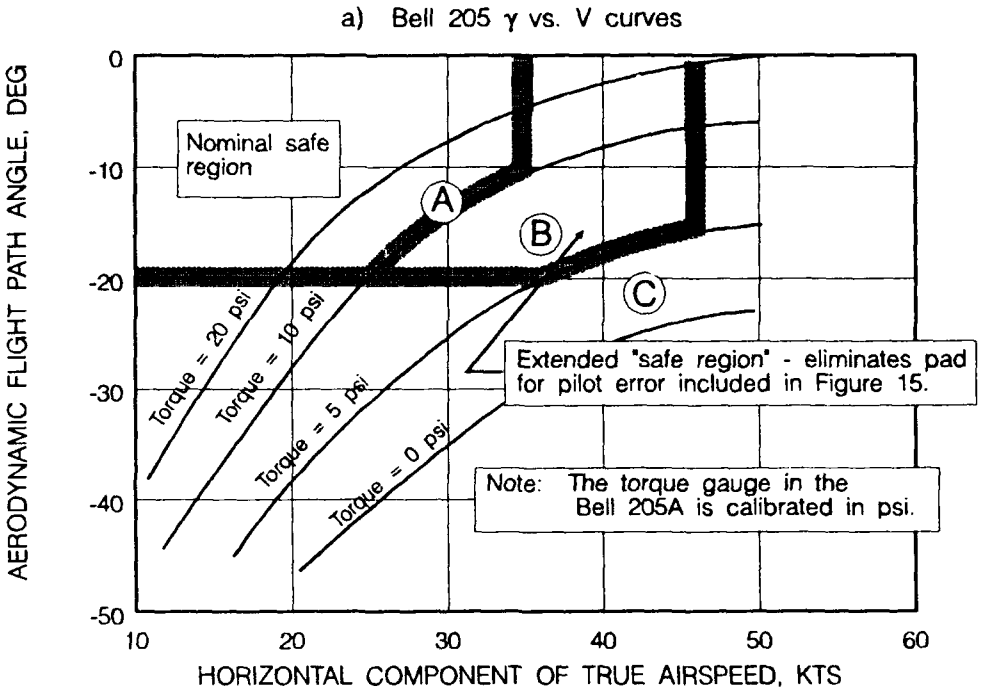

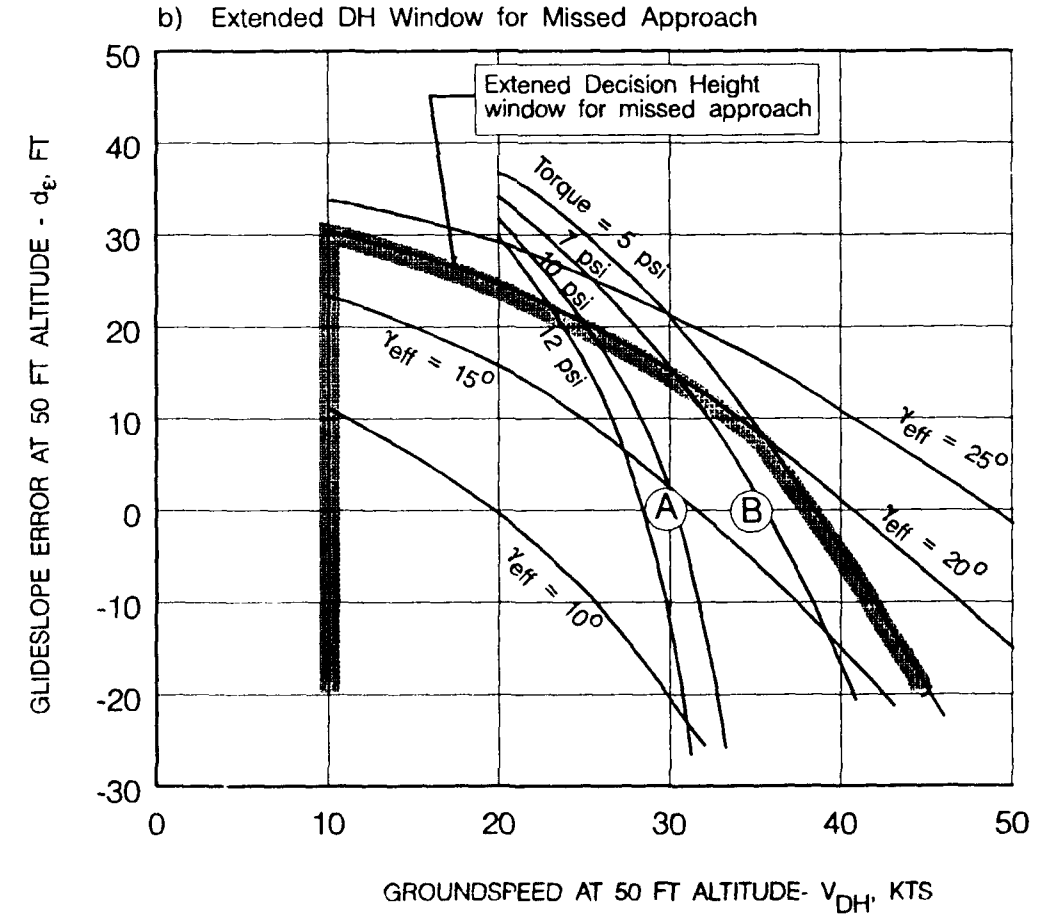

Figure 17. Extended Helicoter Performance Limits Mapped on to d_ε vs. V_{DH} to Obtain DH Window for Missed Approach (γ_o = 9°)

reaching the decision-height point with the landing area in sight, by definition, means that an abort is no longer part of the pilots mental scenario. The overshoot would result in an accident unless there is some "overrun area" i.e., the larger helipad discussed above as rationale for using the extended missed approach DH window.

The point of considering the nominal vs. extended decision height window is not very interesting for the Bell 205A, since it is unlikely that anyone would consider using such an old machine for IMC decelerations to a 50 ft DH. However, it does illustrate that, in general, the missed approach DH window should be based on a margin from the γ -V limits where the helicopter is not comfortable to fly. A more quantitative and generalized definition of such limits will require additional study. Such work is best accomplished in ground-based simulation where the generic characteristics of the rotorcraft can be systematically varied, and operation in marginal regions of the γ - V curves can be safely tested. The DH window for approach coupler and/or flight director requirements should obviously be based on regions of the γ- V curves where the performance and flying qualities are in the desirable range.

D. Effect of Configuration and Glideslope Angle

The effective flight path angle is directly proportional to the glideslope angle, γ_o. This is illustrated by the approximation in Figure 3 where it can be seen that γ_{eff} / γ_o is a function of the glideslope error,, decision height, hover height, and groundspeed at DH. This relationship is plotted in Figure 18, which gives an indication of the variations in window size as a function of γ_{eff} / γ_o. These generic curves indicate that the DH window for missed approach reduces to dimensions which may be unachievable (e.g., glideslope

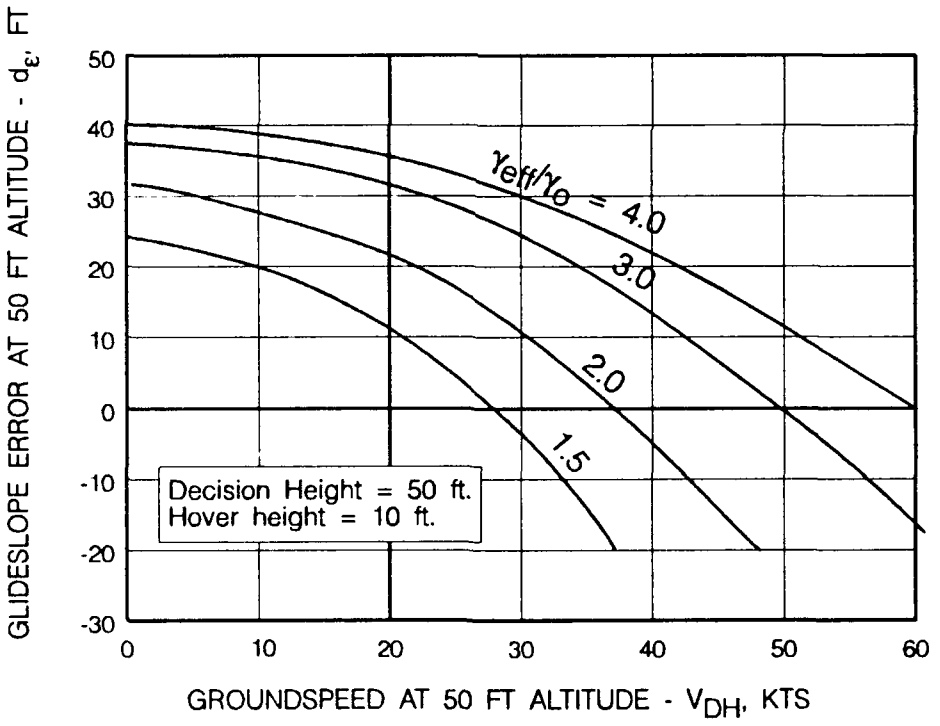

Figure 18. Effect of Systematic Variation of γ_{eff} / γ_o on the Decision-Height Window.

errors of less than 20 ft at 20 kts) when the ratio of the limiting γ_a (and hence γ_{eff}) of the helicopter, to the glideslope angle is equal to or less than 2 (i.e $\gamma_{eff}/\gamma_o \leq 2$). For the Bell 205 this rule of thumb would limit the glideslope angle to $20^o/2 = 10^o$ which is consistent with the experimental results. That is, initial testing indicated that glideslope angles much greater than 9^o were not practical in the Bell 205. Conversely, increasing γ_{eff}/γ_o increases the size of the window. A direct comparison of the Bell 205 missed-approach window dimensions for glideslope angles of 6^o, 9^o, and 12^o is shown in Figure 19. Here it can be seen that the window for a 12 degree glideslope would require very stringent, but not unreasonable approach coupler performance. It is doubtful that the required performance is obtainable with a flight director. Reducing the glideslope angle to 6^o increases the missed-approach DH window dimensions to the point where the flight director of Refs. 6 and 7 would be adequate.

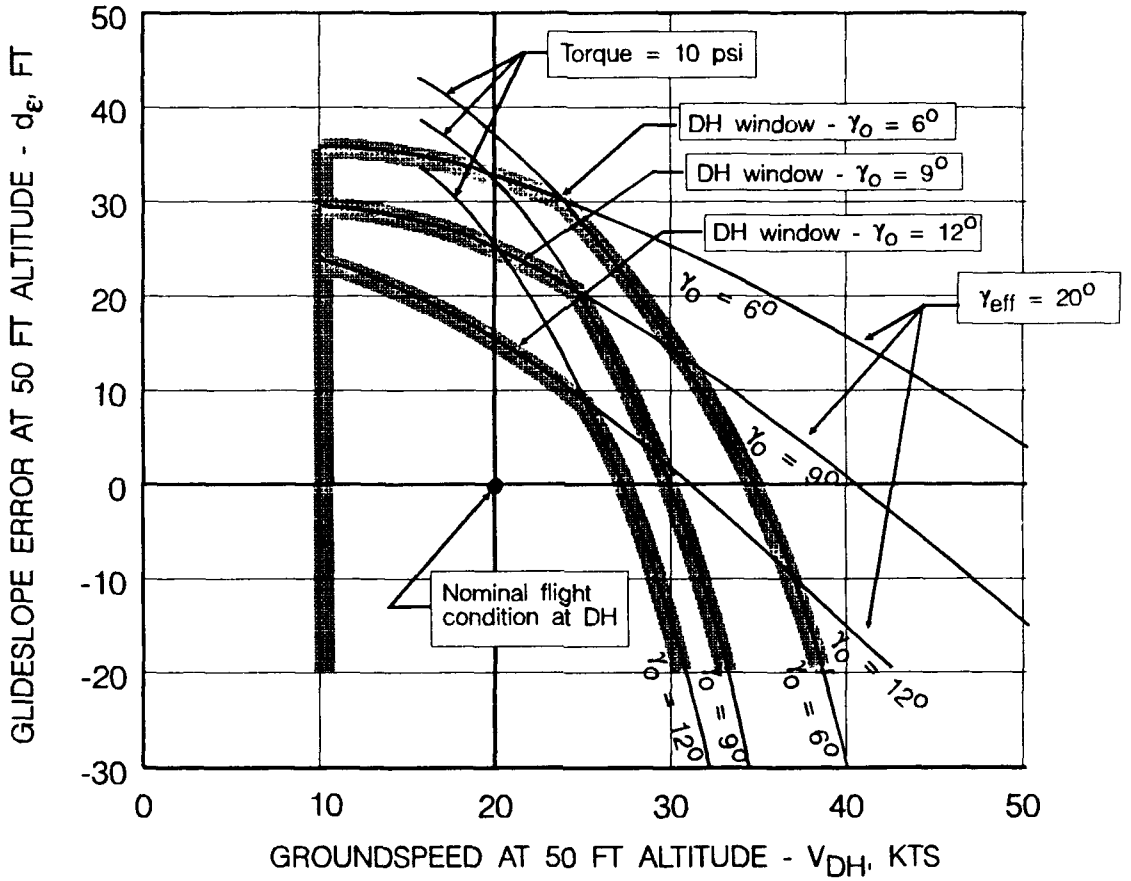

Figure 19. Bell 205A Missed Approach Decision-Height Windows for Three Values of Glideslope Angle.

The few data points obtained for a 6^o glideslope are plotted on the nominal and extended DH window in Figure 20, and tend to confirm the extended window as a definite limit. The DH window for approach coupler design is seen to be conservative for this shallow glideslope as it eliminates three HQRs of 3.

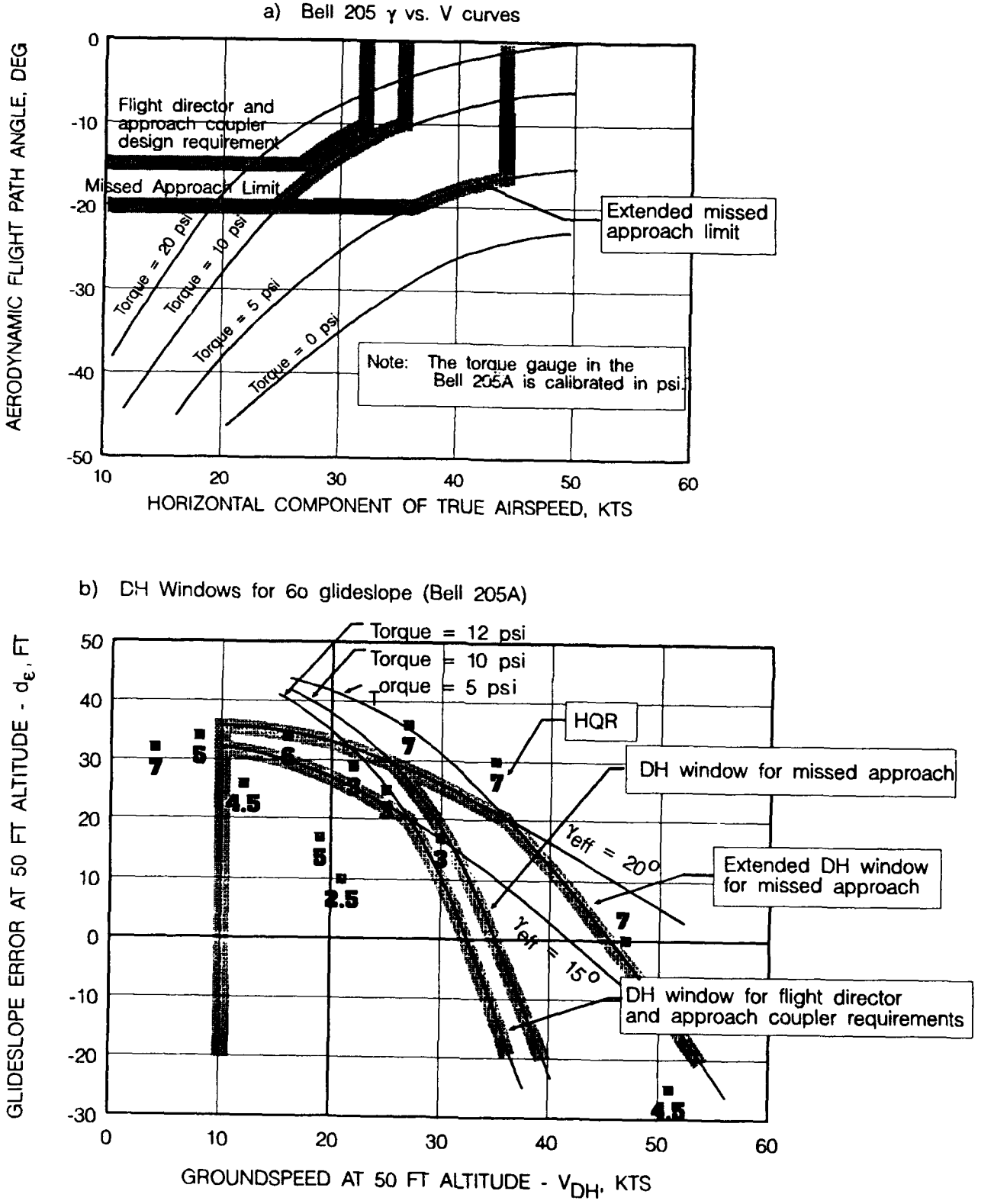

Figure 20. Bell 205A Performance Limits Mapped on to d_ε vs V_{DH} to Obtain DH Windows for Missed Approach and Flight Director/Approach Coupler Requirements (γ_o = 6°).

To gain some insight into the significance of changes in configuration and glideslope angle on the missed-approach DH window dimensions, consider the case of the XV-15 tilt rotor aircraft. For the sake of this example, assume that it has been determined that the XV-15 has acceptable handling qualities and is free from excessive vibration over the following region of its γ- V curves, which have been presented in Figure 4.

$$\gamma_{eff} \leq 40^{o} \text{ -- } V_a \leq 25 \text{ kts}$$
$$\text{Power} \geq 30\% \text{ -- } V_a > 25 \text{ kts}$$

Furthermore, assume that it is desired to use a 20^{o} glideslope to avoid obstructions, and to minimize noise. A final approach speed of 30 kts will be used to maintain at least 30% power, and a sink rate of about 1000 ft/min.[11] The aircraft will be decelerated to a nominal groundspeed of 20 kts at the 50 ft DH, and the nominal hover height is 10 ft. Using the methods discussed above, the DH window shown in Figure 21 results. Here it can be seen that the upper boundary is about the same as it was for the Bell 205 on a 9o glideslope (compare with Figure 15); not surprising since the ratio of γ_{eff}/γ_{o} is about 2 in both cases. The right boundary defined by 30% power is seen to be slightly more restrictive than for the Bell 205.

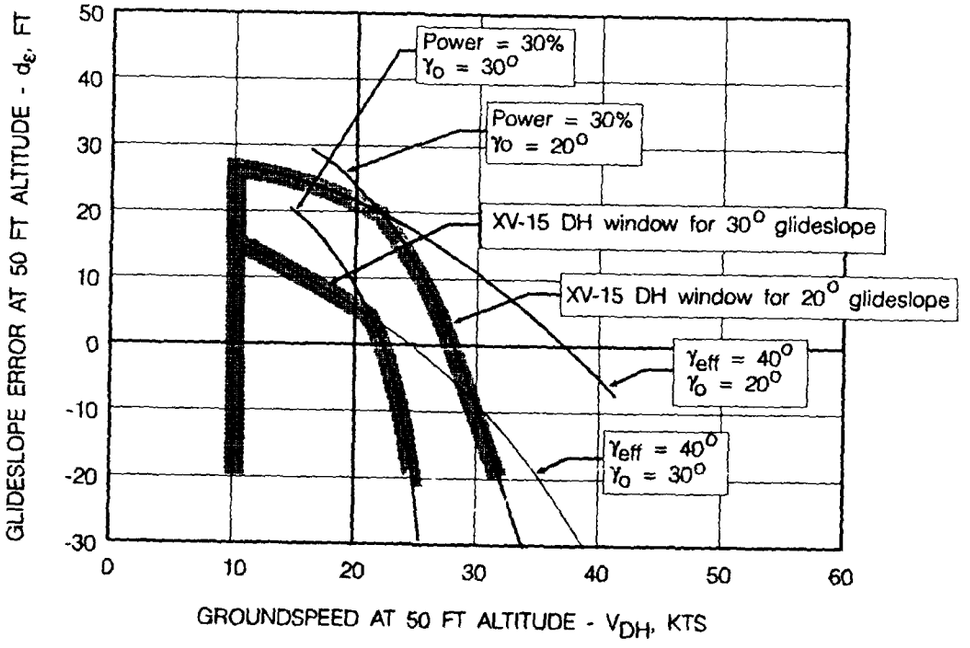

Figure 21. Estimated Decision-Height Windows for the XV-15 Tilt Rotor for Very Steep Glideslope Angles.

[11] It can be seen that steep approach segments must be necessarily short as the required approach speed is very low.

Suppose we now insist on a 30^0 glideslope? This would reduce the ratio of γ_{eff}/γ_0 from 2 to 1.33, which from Figure 18 would be expected to lower the upper boundary considerably. This is verified in Figure 21. Note that the right boundary defined by 30% thrust is also reduced because of the reduction in the ratio of effective flight path angle to glideslope angle. The DH window for a 30^0 glideslope is seen to be exceptionally restrictive. For example, if the helicopter is on glideslope at DH, the groundspeed must be between 10 and 22 kts. It would probably be wise to reduce the nominal DH speed to about 16 kts to provide a symmetrical 6 kt pad. If the aircraft arrives at DH at the target groundspeed of 16 kts, it must not be more than 5 ft high. These limits indicate that for large glideslope angles, the requirements on the rotorcraft and the flight control system will be very stringent. That is, to obtain DH window with dimensions that are consistent with approach coupler and flight director performance capability:

- the aerodynamic flight path angle that can be flown without degradations in handling or excessive vibrations at low speeds, should be at least twice the glideslope angle.
- the minimum power that is practically usable must not result in an overly restrictive right boundary.
- the approach coupler or flight director laws must provide very tight tracking in the presence of all expected winds, wind-shears, and gusts.

Work needs to be done to determine the flight path angle capability of modern rotor systems. The results of the Ref. 6 program would indicate that fully coupled approaches will be necessary for steep flight path angles, unless the flight director deficiencies noted therein can be resolved.

E. Effect of Obscuration After Breakout

As discussed in Section III, a few runs were made to achieve some insight into the effect of visual obscuration, and the resultant degraded cuing after breakout. This was accomplished by setting the fogging level of the electronic goggles so the pad could be seen at DH, but not clearly. This procedure was found to be somewhat unrealistic, as discussed in Section III. However, in the context of obtaining some insight regarding the problem of degraded cuing after breakout, the data for approaches with the goggles fogged from DH to hover are superimposed on the Figure 15, 16, and 17 DH boundaries in Figure 22.

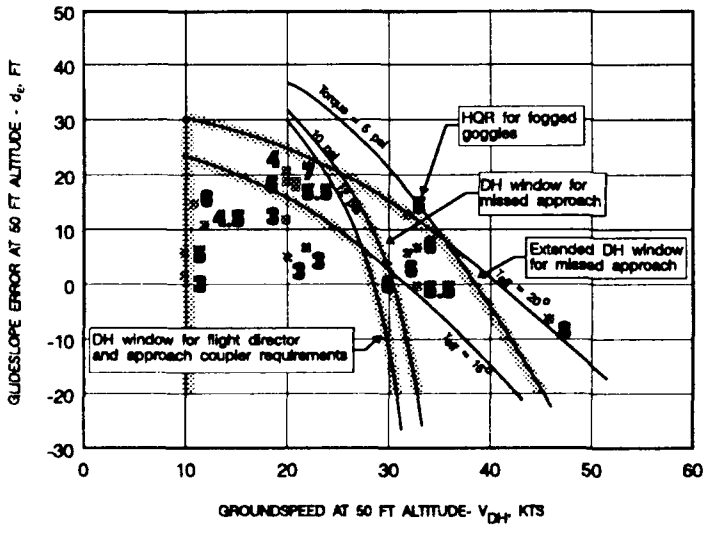

Figure 22 Effect of Degraded Visual Cues on Pilot Ratings for a 9 degree glideslope (Bell 205 Data)

The pilot ratings in the region between the nominal and extended DH windows (i.e., the shaded region in Figure 9) are substantially worse for the fogged runs than for the runs where the goggles cleared at DH (compare Figures 8 and 22). Recall that the physical interpretation of this region is that it only represents a problem if the pilot starts the deceleration to hover late, or applies an incorrect initial control action immediately after DH. With the fogged goggles, this is far more likely than in excellent visibility after DH, and tends to confirm the need for this margin or pad from the helicopter performance limit

defined by the extended DH window. The ratings in the "marginal region" (between the missed approach and approach coupler requirement boundaries) are also somewhat degraded from Figure 8. This may indicate that additional margin is also required for the upper boundary to account for conditions of degraded cuing between DH and hover. Further work is necessary to investigate the effects of approach lighting aids and pad markings to compensate for poor cuing due to degraded visibility after reaching DH.

VI SUMMARY OF RESULTS AND CONCLUSIONS

A methodology has been developed to determine certain critical decision-height window dimensions based on pilot/rotorcraft factors and limitations. Specifically, the method consists of determining the regions of the γ - V performance curves where the rotorcraft flying characteristics are acceptable and mapping these regions onto coordinates that define the DH window (i.e., d_ε vs V_{DH}). This mapping is accomplished via the "effective flight path angle" parameter or γ_{eff}.

Insights and initial estimates of the DH window dimensions have been obtained from an exploratory flight test program with the Canadian NRC variable stability Bell 205. These results are summarized below.

- The upper and right boundaries of the DH window are based on helicopter performance limits.
- The left boundary of the DH window is based on rotorcraft handling at very low airspeeds.
- The bottom boundary of the DH window is based on obstruction avoidance, and pad visibility. This boundary is not affected by rotorcraft performance or handling qualities.
- The right boundary of the DH window is based on the minimum usable torque (power), and related maximum acceptable pitch attitude during deceleration. Some margin is required to account for pilot delay in initiating the deceleration after breakout.
- The upper boundary of the DH window is based on the maximum aerodynamic flight path angle that can be flown at low airspeeds. It requires some margin for pilot delay or control misapplication in conditions of poor visual cuing, but is less critical in this regard than the right boundary.
- Simulation of poor visual cuing after breakout emphasized the need for margin from rotorcraft performance limits for both the right and upper DH window boundaries.
- The dimensions of the DH window are directly proportional to the ratio of the maximum usable aerodynamic flight path angle (i.e., γ_{eff}) to the glideslope angle (γ_o). As a rule-of-thumb, values of $\gamma_{eff}/\gamma_o \leq 2$ result in DH window dimensions that would be difficult to achieve consistently with existing flight hardware in a variety of wind and windshear conditions.

The DH window dimensions obtained from considerations of pilot/rotorcraft factors and limitations should be superimposed on other operational considerations such as field-of-view, airspace availability, available real estate for helipad and approach lighting, obstructions, noise, etc. The ultimate decision on setting the window dimensions should be based on certification flight testing on a case-by-case basis. The results of this study, and any future studies, should provide a basis for setting reasonable window dimensions prior to such testing.

VII REFERENCES

1. Enias, James H., Course Width Determination for Collocated MLS at Heliports, DOT/FAA/CT-TN85/15, December 1985.

2. Weiss, Rosanne M., Christopher J. Wolf, et. al., Heliport Visual Approach and Departure Airspace Tests, Vol 1 Summary, DOT/FAA/CT-TN87/40, I, August 1988.

3. Baillie, Stewart. W., Stan. Kereliuk, R. Srinivassan, and Roger Hoh, Tracking Performance Requirements for Rotorcraft Instrument Approaches to Reduced Minima, Institute for Aerospace Research, National Research Council of Canada, Aeronautical Note IAR-AN-70, NRC No. 32137, February, 1991.

4. Washizu, Kyuichiro, Akira Azuma, Experiments on a Model Helicopter Rotor Operating in the Vortex Ring State, AIAA Journal of Aircraft, Vol. 3, No. 3, June 1966.

5. Hoh, Roger H., Investigation of the Vulnerability of Powered Lift STOL's to Wind Shear, AIAA Paper 11-1120, August 1977.

6. Hoh, Roger H., Stewart Baillie, and Stan Kereliuk, Flight Test Investigation of Flight Director and Autopilot Functions for Helicopter Decelerating Instrument Approaches, DOT/FAA/CT-TN89/54, January 1989.

7. Baillie, S., S. Kereliuk, and R. Hoh, An Investigation of Lateral Tracking Techniques, Flight Directors and Automatic Control Coupling on Decelerating IFR Approaches for Rotorcraft, Aeronautical Note NAE AN-55, NRC No. 29604, National Aeronautical Establishment, Ottawa Canada, October 1988.

8. Hoh, Roger H., A Review of Certain Generic Characteristics of the 3-Cue Flight Director for Decelerating Instrument Approaches in Helicopters, DOT/FAA/CT-TN90/5, December 1989.

APPENDIX A

SUMMARY OF PILOT RATINGS AND COMMENTARY

The pilot ratings for this experiment are summarized in Tables A-1 and A-2. These tables are identical except that the data is sorted by approach number in Table A-1 and by HQR in Table A-2. These sortings have been found to be useful for correlating the data plots with the pilot commentary which is summarized below.

APPROACH NUMBER	PILOT COMMENTARY
1	Overshot pad by about 50 ft. Maxed out on θ and down collective. Barely saw pad under nose at breakout. Lost pad during deceleration; θ at about 20 degrees.
2	Never saw pad clearly. Came to hover open loop about 20 ft long and 20 ft left of pad. Winds at 400 ft were approximately 25 kts headwind.
3	No problem
4	No problem
5	Overshot pad - θ too high for this maneuver - might have been a little late on pitch up (flare) - HQR = 7 due to attitude and collective inputs.
6	No problem
7	No problem
8	Coupled collective and attitude and flew bank angle manually during IMC portion of approach. Required θ not bad (acceptable), but required collective seemed excessive. Flared high - pad visibility fair; could see out of side. Stopped at far end of pad - seemed slow at breakout. Forgot to disengage autopilot at first, resulting in a delay.
9	Manual approach in IMC conditions. No problem. Did not feel rushed - pad visibility good.
10	Tower winds 250 deg at 20 kts - θ and collective activity not a problem, but just below where it gets to be a problem. Pad visibility good - not rushed. Manual approach in IMC conditions. Manual approach is easier - turning autopilot off is a big transition at a critical time.
11	Good - a little high.
12	High and slow - noticeable vibration, but not a primary factor (yet). Steep approach; close to borderline steep, vibration was a factor - near vortex ring state - uncomfortable.

13 Rapid deceleration - close to maximum effort - flare was extreme - could not see far end of pad - used side of pad for guidance.

14 No good - stopped 50 ft past pad - used maximum θ and held it.

15 A little high at breakout, but not a problem. θ and collective ok - vibration somewhat annoying, but not severe. Lateral ok - urgency, none - pad visibility good.

16 A fair bit of up collective required - no problem.

17 Slow deceleration - slight vibration - uncomfortable.

18 Same as above.

19 Another slow deceleration - more vibration - pitch flight director gave problems at bread-out - still acceptable.

20 Closure rate too high - went to maximum θ and minimum collective. Altitude not a problem. Urgency was excessive. Overshot pad by one or two helicopter lengths - no vibration - line-up was good.

21 Breakout was high and slightly left of pad. Fairly large θ and collective, but not excessive. Terminate near center of pad. Urgency was moderate - vibration was slight.

22 Somewhat high at break-out - on localizer - no problem - urgency was slight - vibration was slight.

23 Break-out high and left - able to make pad without excessive urgency (urgency judged as moderate). Some delay (1 to 2 sec) finding pad. θ and collective activity were moderate - right sidestep was a factor - vibration was not a factor - wind was from left.

24 No go! Low on glideslope, but too fast.

25 Ok - rapid deceleration and large positive δ_c - workload high - acceptable.

26 A bit steep - vibration noticeable - getting closer to borderline.

27 Steep descent - moderate vibrations - high workload - reduced visibility would cause problems - h/v curve violation ?? - borderline.

28 θ and collective activity moderately high - not pleasant, but acceptable. Pad visibility only fair-to-poor. Urgency was moderate. Vibrations were objectionable. Line-up was good.

29 θ and collective requirements were excessive - urgency was high - rapid closure with pad, offset to right - stopped on far right corner - Tower winds were 120 degrees at 10 kts.

30 Fairly aggressive θ, but acceptable - urgency between slight and moderate - tower winds were 090 variable 120 at 5 to 10 kts. Some vibration, but acceptable.

31 Closure rate very high - max acceptable θ and a lot of collective activity - urgency was extreme - wind 110 deg at 10 kts (tower) - pad visibility was ok.

32 Very high on break-out, but pad visibility was ok. Vibration was excessive. Terminated at center of pad following very steep approach. HQR = 6 mainly due to vibration. Any higher would have been unacceptable. Low groundspeed saved the approach.

33 No good - went by pad by about 100 ft.

34 Same as above.

35 Steep and very slow - moderate vibrations and "bucking" - uncomfortable, but acceptable.

36 Steep and very slow - vibration and "bucking" - ended up 100 ft short of pad - excessive δ_c required. Collective workload very high - too steep and slow.

37 Very similar to above - collective flight director followed diligently - back end of pad - too steep and slow.

38 Almost nominal - slightly fast and high

39 Slightly fast and quite high - ended up in back 50% of pad - no vibration - quite steep - possible visibility problems.

40 No real problems with height - speed seemed low - vibration noticed - stopped 100 ft short.

41 A bit fast - flare and stop easy, accurate.

42 Fast and high - ended up 100 ft past the pad - too aggressive a flare required.

43 Same as above - went past by 150 ft.

44 Fast and high - stopped at back of pad - excessive θ - borderline but acceptable.

45 Overshot pad by 100 ft.

46 A little fast but no problem.

47 almost an overshoot - by 2 ft.

48 Same as above.

49 High and slow - might be a problem in poor visibility.

50	Same as above.
51	Aggressive flare required.
52	Very interesting - very easy approach.
53	Like the last one - some θ required to flare.
54	A bit aggressive in the flare - watch for poor visibility case - not borderline.
55	Acceptable - broke out slightly to the right - stopped at pad center.
56	Went by pad by 150 ft. Had problems with guidance during deceleration in IMC conditions.
57	Went way past pad. Had problems with guidance during deceleration in IMC conditions.
58	No way to stop before fence (about 200 ft beyond pad).
59	Like approach 55 - stopped at far end of pad - limit of acceptable.
60	New flight director - definitely borderline - guidance problems during IMC deceleration.
61	Almost made it - just into the unacceptable region - over pad boundary at far end.
62	A good one.
63 - 68	Very strong crosswinds from the right side with big shear at 400 ft agl. Very unpleasant.
63	No problem - some vibration, but not excessive - good position and speed.
64	No problem in transition - shear makes it very difficult to track speed and glideslope during deceleration - approximately 10 degrees into wind offset used this time (reference to wing low technique during IMC tracking) - too tough on airframe otherwise.
65	Very easy - gentle pitch correction and deceleration - noticeably steeper than last two approaches.
66	Less time available, but still no problem - aircraft position and speed was excellent - slight use of pitch and progressive up-collective was all that was needed. Don't want to down-rate because of approach conditions, but cross-wind and sun make it very difficult.
67	Steep but slow - transitional vibration before 50 feet which stopped almost as the goggles cleared - from 50 feet on down had absolutely no problem.

68	Seemed like run 65 - same comments and rating.
69	Fast but ok - time short but set-up good so no problem.
70	Very fast - not able to stop within confines of the pad using as much attitude as I was prepared to do.
71	Fast but ok - very good set-up - moderate θ - not Level 1 - I had insufficient time to end up exactly where I wanted to be.
72	Slower but close in - no problem - good set-up - broken goggles distracting down approach - affected tracking.
73	Fast high and close - 1/2 fuselage beyond pad - HQR based on performance.
74	Moderate speed but very high - difficult to spot pad but Tx ok - ended up inside pad but not at the spot of choice.
75	High and fast - 3/4 fuselage length beyond pad.
76	Vibrations - slight problem seeing pad.
77	Same comments as above - plenty of time to stop however.
78	Difficult to tell when glasses unfog - high sink at bottom - made pad but power application intolerable.
79	Large flare - intolerable
80	High - made the pad, but nearly lost sight of it under the nose of the aircraft.
81	Broke out short and high - took a few seconds to acquire pad under the nose which was high (pitched-up) - vibrations in close.
82	Some vibrations, but not particularly objectionable - easy acquisition of pad.
83	Large overshoot of pad (50 plus feet) - late in power application.
84	Past pad by 10 feet - large flare.
85	Stopped short - taxied to pad.
86	50 to 75 feet overshoot.
87	Some vibrations, but acceptable - acquiring pad took a little time - power and control manipulations within acceptable range.
88	25 foot overshoot - not uncomfortable at bottom, but clearly unable to make pad with maximum acceptable flare.

89 Fairly large flare, but not unreasonable.

90 Made the pad but aircraft was gyrating fairly heavy upon power application - controllability not an issue.

91 Stopped high and short - did not break out initially - when power reduced, broke out and settled straight down to spot - flight director was calling for reduced power.

92 Same general comments as above, but stayed with flight director - not as close to a "7" as above; lots of gyrating during out-of-ground-effect hover portion of approach.

93 Made the spot, but very uncomfortable - high power - steep in close - nearly missed visual acquisition of the pad - reluctant to lower power per flight director cue.

94 25 feet beyond pad - too fast - no way - too high.

95 Good - no attitude change to the pad.

96 Steep slow approach - vibrations - could be a problem in poor visibility.

97 Slight flare required - could have easily stopped in center of pad.

98 Steep slow approach - vibrations slight - could be a problem in low visibility.

99 Steep and slow - short of pad by 100 ft.

100 A bit steep but ok.

101 No comments.

102 High - could be a problem with poor visibility.

103 Fast but low.

104 Just past pad by 25 feet - just past limit - could not see pad.

105 Same as above - high θ - just past pad by 25 feet.

106 No joy - 50 ft hover - galloping

107 High and hot - just past pad by 25 feet - high θ.

Remainder of runs are with fogged goggles all the way to hover to simulate reduced visibility after break-out.

108 Height cues very bad - Break out right - lucked-out finding pad - lost it in height - safety pilot took over.

109 Ditto - Closure rate and θ were problems - black ice at center of pad saved me - Acceptable.

110 Workload high - poor height cues - borderline but acceptable.

111 Very rapid flare - high θ - aggressive - acceptable but borderline.

112 Goggles set to 1/8 mile - right 90 deg crosswind based on windsock (tower winds 310 deg at 10 kt). Pad visibility fair-to-poor - urgency slight - closure rate and sink-rate difficult to pick up but possible. Stopped past right center of pad.

113 High on break-out - stopped at far end. Urgency moderate-to-high - difficult to tell what to do. Not even sure how I did; asked safety pilot - Need more detail on pad. δ_c and θ near maximum for these cues.

114 No problem - could see all cones defining pad - urgency; none - stopped at center of pad.

115 Fast at breakout - urgency high - stopped on centerline, but just inside back boundary of pad. θ was at max value and I was uncertain of altitude and altitude rate in flare. Unacceptable.

116 Winds 280 deg at 8 kts (tower). No problem.

117 Very rapid deceleration at maximum θ - problems with altitude cues but not sink-rate. Approaching borderline.

118 Slow - vibrations significant - approach easy - HQR = 5 due to vibration, otherwise a 3.

119 Slow and steep - moderate vibration - height cues were bad.

120 Urgency very high - unacceptable - extreme θ - lot of collective to assist in braking and to assure that altitude is ok. Lost pad in flare. Problem with goggles due to sun in eyes. Flared to high hover (estimate 25 ft).

121 Too fast at breakout - very large θ, but still not possible to stop over pad, stayed high attempting to bleed speed - stopped two fuselage lengths past pad - visibility not a factor.

122 No problem.

123 Broke out far from pad - had problem finding at first - sun is a big factor - no problem once pad in sight.

124 High at breakout - required θ moderately high - sense of urgency moderate - acceptable but borderline.

Table A-1. Pilot Rating Data and Effective Flight Path Angle Calculations (Sorted by Approach Number)

APP #	FLIGHT	PILOT	DEPS	VDH	WIND	R	RS	GAMAF	GAMAEFF	NWGAMAEFF	HQR	GS ANGLE
1	20	RH	5	48	-15	284.14	286.94	8.01	27.55	29.71	7	9
2	20	RH	7	36	-15	271.51	274.44	8.38	18.21	20.81	7	9
3	20	SK	-8	12	-15	366.23	368.40	6.23	3.77	7.23	3	9
4	20	SK	-1	11	-15	322.03	324.50	7.08	3.94	8.04	3	9
5	20	SK	-4	36	-15	340.97	343.31	6.69	14.47	16.50	7	9
6	20	SK	3	12	-15	296.77	299.45	7.68	4.64	8.91	3	9
7	20	SK	-1	29	-15	322.03	324.50	7.08	11.32	13.78	4	9
8	21	RH	25	14	-15	157.86	162.84	14.22	9.96	17.40	4.5	9
9	21	RH	11	22	-15	246.25	249.48	9.23	10.47	14.26	2.5	9
10	21	RH	-26	33	-15	479.88	481.55	4.77	9.06	10.57	3	9
11	21	SK	9	23	-15	258.88	261.96	8.78	10.50	14.02	3	9
12	21	SK	24	14	-15	164.17	168.97	13.69	9.59	16.75	5	9
13	21	SK	17	23	-15	208.37	212.17	10.87	13.01	17.40	6	9
14	21	SK	14	35	-15	227.31	230.80	9.98	20.92	24.12	7	9
15	22	RH	14	16	4	227.31	230.80	9.98	16.18	12.86	2.5	9
16	22	SK	-10	37	4	378.85	380.96	6.03	16.08	15.33	4	9
17	22	SK	8	23	4	265.20	268.20	8.58	15.52	13.69	3	9
18	22	SK	19	17	4	195.74	199.79	11.55	18.90	15.33	3	9
19	22	SK	24	18	4	164.17	168.97	13.69	22.72	18.77	4	9
20	23	RH	0	43	0	315.71	318.24	7.22	22.54	22.54	7	9
21	23	RH	1	32	0	309.40	311.97	7.37	15.89	15.89	4.5	9
22	23	RH	15	19	0	221.00	224.59	10.26	14.44	14.44	3	9
23	23	RH	26	14	0	151.54	156.73	14.79	18.10	18.10	4.5	9
24	23	SK	-2	45	0	328.34	330.77	6.95	23.11	23.11	7	9
25	23	SK	5	35	0	284.14	286.94	8.01	19.19	19.19	4	9
26	23	SK	14	23	0	227.31	230.80	9.98	15.96	15.96	5	9
27	23	SK	30	12	0	126.28	132.47	17.58	20.50	20.50	6	9
28	24	RH	14	27	4.5	227.31	230.80	9.98	20.32	18.26	5	9
29	24	RH	14	37	6.5	227.31	230.80	9.98	28.20	25.87	7	9
30	24	RH	-11	32	6.5	385.17	387.24	5.93	14.28	12.74	4	9
31	24	RH	-2	45	11	328.34	330.77	6.95	25.54	23.11	8	9
32	24	RH	35	14	10	94.71	102.81	22.90	75.08	28.27	6	9
33	24	SK	19	32	10	195.74	199.79	11.55	30.98	25.31	7	9
34	24	SK	7	41	10	271.51	274.44	8.38	27.62	24.67	7	9
35	27	SK	31	13	0	119.97	126.46	18.44	22.06	22.06	5.5	9
36	27	SK	5	8	0	284.14	286.94	8.01	8.59	8.59	7	9
37	27	SK	35	14	0	94.71	102.81	22.90	28.27	28.27	7	9
38	27	SK	14	20	0	227.31	230.80	9.98	14.49	14.49	3	9
39	27	SK	24	20	0	164.17	168.97	13.69	19.98	19.98	4	9
40	28	SK	-2	9	-14	328.34	330.77	6.95	3.34	7.57	4	9
41	28	SK	18	23	-12	202.06	205.98	11.20	14.01	17.95	3	9
42	28	SK	18	34	-15	202.06	205.98	11.20	22.60	26.30	7	9
43	28	SK	33	33	-11	107.34	114.55	20.44	43.37	50.43	7	9
44	28	SK	3	41	-14	296.77	299.45	7.68	20.41	22.49	6	9
45	28	SK	34	31	-12	101.03	108.66	21.60	41.42	49.50	7	9
46	29	MM	24	22	-12	164.17	168.97	13.69	16.33	21.33	4	9
47	29	MM	0	10	-12	315.71	318.24	7.22	4.08	8.03	4	9
48	29	MM	13	10	-12	233.63	237.03	9.72	5.49	10.81	4.5	9
49	30	SK	28	15	-13	138.91	144.56	16.06	12.64	20.23	4	9
50	30	SK	24	21	-13	164.17	168.97	13.69	15.25	20.64	3	9
51	30	SK	25	27	-11	157.86	162.84	14.22	21.98	26.37	5	9
52	30	SK	22	14	-10	176.80	181.27	12.75	10.22	15.58	2.5	9
53	30	SK	20	22	-10	189.43	193.60	11.92	14.69	18.51	3	9
54	30	SK	21	26	-12	183.11	187.43	12.32	17.86	21.92	5.5	9
55	31	SK	16	25	0	214.68	218.38	10.56	18.07	18.07	4	9
56	31	SK	28	35	0	138.91	144.56	16.06	40.74	40.74	7	9
57	31	SK	20	49	0	189.43	193.60	11.92	49.17	49.17	9	9
58	31	SK	22	62	0	176.80	181.27	12.75	ERR	ERR	9	9
59	31	SK	26	27	0	151.54	156.73	14.79	27.49	27.49	6	9
60	31	SK	29	26	0	132.60	138.50	16.79	30.35	30.35	4	9
61	32	SK	4	40	0	290.45	293.20	7.84	22.24	22.24	7	9
62	32	SK	7	23	0	271.51	274.44	8.38	13.37	13.37	2.5	9
63	36	MM	-8	23	-5	366.23	368.40	6.23	8.80	9.92	2.5	9
64	36	MM	-5	25	-10	347.28	349.58	6.57	9.27	11.17	2	9
65	36	MM	-1	29	-7	322.03	324.50	7.08	12.72	13.78	3	9
66	36	MM	15	13	-5	221.00	224.59	10.26	7.73	12.21	2	9
67	36	MM	13	18	-5	233.63	237.03	9.72	10.52	13.26	2	9
68	36	MM	14	24	-10	227.31	230.80	9.98	14.74	16.50	2.5	9
69	37	MM	1	31	-22	309.40	311.97	7.37	14.31	15.36	3	9

Table A-1. Pilot Rating Data and Effective Flight Path Angle Calculations (Sorted by Approach Number) - (Concluded)

APP #	FLIGHT	PILOT	DEPS	VDH	WIND	R	RS	GAMAF	GAMAEFF	NWGAMAEFF	HQR	GS ANGLE
70	37	MM	-3	47	-27	334.65	337.04	6.82	22.87	24.17	7	9
71	37	MM	1	38	-23	309.40	311.97	7.37	16.66	19.48	4	9
72	37	MM	17	24	-26	208.37	212.17	10.87	12.10	18.00	2.5	9
73	37	MM	23	36	-25	170.48	175.11	13.21	27.94	33.83	7	9
74	37	MM	31	19	-25	119.97	126.46	18.44	15.18	26.29	4.5	9
75	37	MM	25	32	-22	157.86	162.84	14.22	24.70	31.64	7	9
76	41	EB	-1	21	0	322.03	324.50	7.08	9.44	10.58	4	9
77	41	EB	-8	26	0	366.23	368.40	6.23	10.11	10.95	4	9
78	41	EB	-4	32	0	340.97	343.31	6.69	14.41	14.41	7	9
79	41	EB	19	22	0	195.74	199.79	11.55	17.92	17.92	5	9
80	41	EB	28	18	0	138.91	144.56	16.06	22.09	22.09	6	9
81	41	EB	31	6	0	119.97	126.46	18.44	19.20	19.20	4	9
82	41	EB	8	4	5	265.20	268.20	8.58	29.73	8.73	4	9
83	42	EB	34	26	8	101.03	108.66	21.60	51.73	40.10	7	9
84	42	EB	15	33	9	221.00	224.59	10.26	27.25	23.15	7	9
85	42	EB	4	10	0	290.45	293.20	7.84	8.72	8.72	4	9
86	42	EB	10	38	0	252.57	255.72	9.00	24.01	24.01	7	9
87	42	EB	37	11	4	82.08	91.31	25.98	43.78	29.79	5	9
88	42	EB	-1	40	4	322.03	324.50	7.08	20.83	20.00	7	9
89	43	EB	4	25	0	290.45	293.20	7.84	13.35	13.35	5	9
90	43	EB	25	17	0	157.86	162.84	14.22	18.93	18.93	6	9
91	43	EB	44	6	9	37.89	55.09	46.56	44.04	49.03	7	9
92	43	EB	36	8	7	88.40	97.03	24.35	ERR	26.20	6	9
93	43	EB	30	16	5	126.28	132.47	17.58	30.79	22.81	6	9
94	43	EB	24	23	3	164.17	168.97	13.69	24.19	22.06	7	9
95	39	SK	10	21	3	380.60	382.70	6.00	9.96	8.95	2.5	6
96	39	SK	34	16	4	152.24	157.41	14.72	23.96	19.04	6	6
97	39	SK	17	30	0	314.00	316.53	7.26	14.62	14.62	3	6
98	39	SK	34	8	0	152.24	157.41	14.72	15.79	15.79	5	6
99	39	SK	17	19	0	314.00	316.53	7.26	10.19	10.19	5	6
100	39	SK	29	22	0	199.82	203.78	11.32	17.56	17.56	3	6
101	39	SK	25	25	0	237.88	241.22	9.55	16.31	16.31	3	6
102	39	SK	26	12	0	228.36	231.84	9.94	11.54	11.54	4.5	6
103	40	SK	-25	51	-4	713.63	714.75	3.21	12.32	12.55	4.5	6
104	40	SK	36	27	-4	133.21	139.09	16.71	28.96	31.34	7	6
105	40	SK	0	47	-4	475.75	477.43	4.81	16.41	16.80	7	6
106	40	SK	32	4	-4	171.27	175.88	13.15	6.81	13.38	7	6
107	40	SK	30	35	-4	190.30	194.46	11.87	27.67	29.02	7	6
108	25	SK-FOG	19	21	-4	195.74	199.79	11.55	15.46	17.35	7	9
109	25	SK-FOG	4	30	-4	290.45	293.20	7.84	14.87	15.82	6	9
110	25	SK-FOG	19	20	-4	195.74	199.79	11.55	14.84	16.80	6	9
111	25	SK-FOG	15	11	-4	221.00	224.59	10.26	8.91	11.65	6	9
112	25	RH-FOG	21	20	-4	183.11	187.43	12.32	15.85	17.94	4	9
113	25	RH-FOG	13	32	-4	233.63	237.03	9.72	19.99	21.12	5	9
114	25	RH-FOG	12	20	-4	239.94	243.25	9.47	12.14	13.73	3	9
115	25	RH-FOG	6	32	-4	277.83	280.69	8.19	16.78	17.72	6	9
116	26	SK-FOG	5	20	-6	284.14	286.94	8.01	9.74	11.61	3	9
117	26	SK-FOG	0	33	-6	315.71	318.24	7.22	14.97	16.11	5.5	9
118	26	SK-FOG	6	10	-6	277.83	280.69	8.19	6.03	9.11	5	9
119	26	SK-FOG	11	12	-6	246.25	249.48	9.23	7.63	10.72	4.5	9
120	26	RH-FOG	7	33	-6	271.51	274.44	8.38	17.43	18.77	6	9
121	26	RH-FOG	-6	46	-6	353.60	355.85	6.45	21.30	22.10	8	9
122	26	RH-FOG	7	22	-6	271.51	274.44	8.38	11.13	12.94	3	9
123	26	RH-FOG	2	10	-6	303.08	305.71	7.52	5.54	8.36	3	9
124	26	RH-FOG	18	21	-6	202.06	205.98	11.20	14.27	16.81	5.5	9

Table A-2. Pilot Rating Data and Effective Flight Path Angle Calculations (Sorted by HQR)

APP #	FLIGHT	PILOT	DEPS	VDH	WIND	R	RS	GAMAF	GAMAEFF	NWGAMAEFF	HQR	GS ANGLE
64	36	MM	-5	25	-10	347.28	349.58	6.57	9.27	11.17	2	9
66	36	MM	15	13	-5	221.00	224.59	10.26	12.21	12.21	2	9
67	36	MM	13	18	-5	233.63	237.03	9.72	9.76	13.26	2	9
9	21	RH	11	22	-15	246.25	249.48	9.23	10.47	14.26	2.5	9
15	22	RH	14	16	4	227.31	230.80	9.98	16.18	12.86	2.5	9
52	30	SK	22	14	-10	176.80	181.27	12.75	10.22	15.58	2.5	9
62	32	SK	7	23	0	271.51	274.44	8.38	13.37	13.37	2.5	9
63	36	MM	-8	23	-5	366.23	368.40	6.23	8.80	9.92	2.5	9
68	36	MM	14	24	-10	227.31	230.80	9.98	16.50	16.50	2.5	9
72	37	MM	17	24	-26	208.37	212.17	10.87	16.07	18.00	2.5	9
3	20	SK	-8	12	-15	366.23	368.40	6.23	3.77	7.23	3	9
4	20	SK	-1	11	-15	322.03	324.50	7.08	3.94	8.04	3	9
6	20	SK	3	12	-15	296.77	299.45	7.68	4.64	8.91	3	9
10	21	RH	-26	33	-15	479.88	481.55	4.77	9.06	10.57	3	9
11	21	SK	9	23	-15	258.88	261.96	8.78	10.50	14.02	3	9
17	22	SK	8	23	4	265.20	268.20	8.58	15.52	13.69	3	9
18	22	SK	19	17	4	195.74	199.79	11.55	18.90	15.33	3	9
22	23	RH	15	19	0	221.00	224.59	10.26	14.44	14.44	3	9
38	27	SK	14	20	0	227.31	230.80	9.98	14.49	14.49	3	9
41	28	SK	18	23	-12	202.06	205.98	11.20	14.01	17.95	3	9
50	30	SK	24	21	-13	164.17	168.97	13.69	15.25	20.64	3	9
53	30	SK	20	22	-10	189.43	193.60	11.92	14.69	18.51	3	9
65	36	MM	-1	29	-7	322.03	324.50	7.08	11.55	13.78	3	9
69	37	MM	1	31	-22	309.40	311.97	7.37	13.52	15.36	3	9
7	20	SK	-1	29	-15	322.03	324.50	7.08	11.32	13.78	4	9
16	22	SK	-10	37	4	378.85	380.96	6.03	16.08	15.33	4	9
19	22	SK	24	18	4	164.17	168.97	13.69	22.72	18.77	4	9
25	23	SK	5	35	0	284.14	286.94	8.01	19.19	19.19	4	9
30	24	RH	-11	32	6.5	385.17	387.24	5.93	14.28	12.74	4	9
39	27	SK	24	20	0	164.17	168.97	13.69	19.98	19.98	4	9
40	28	SK	-2	9	-14	328.34	330.77	6.95	3.34	7.57	4	9
46	29	MM	24	22	-12	164.17	168.97	13.69	16.33	21.33	4	9
47	29	MM	0	10	-12	315.71	318.24	7.22	4.08	8.03	4	9
49	30	SK	28	15	-13	138.91	144.56	16.06	12.64	20.23	4	9
55	31	SK	16	25	0	214.68	218.38	10.56	18.07	18.07	4	9
60	31	SK	29	26	0	132.60	138.50	16.79	30.35	30.35	4	9
71	37	MM	1	38	-23	309.40	311.97	7.37	19.48	19.48	4	9
76	41	EB	-1	21	0	322.03	324.50	7.08	7.60	10.58	4	9
77	41	EB	-8	26	0	366.23	368.40	6.23	8.65	10.95	4	9
81	41	EB	31	6	0	119.97	126.46	18.44	19.20	19.20	4	9
82	41	EB	8	4	5	265.20	268.20	8.58	29.73	8.73	4	9
85	42	EB	4	10	0	290.45	293.20	7.84	8.72	8.72	4	9
8	21	RH	25	14	-15	157.86	162.84	14.22	9.96	17.40	4.5	9
21	23	RH	1	32	0	309.40	311.97	7.37	15.89	15.89	4.5	9
23	23	RH	26	14	0	151.54	156.73	14.79	18.10	18.10	4.5	9
48	29	MM	13	10	-12	233.63	237.03	9.72	5.49	10.81	4.5	9
74	37	MM	31	19	-25	119.97	126.46	18.44	26.29	26.29	4.5	9
12	21	SK	24	14	-15	164.17	168.97	13.69	9.59	16.75	5	9
26	23	SK	14	23	0	227.31	230.80	9.98	15.96	15.96	5	9
28	24	RH	14	27	4.5	227.31	230.80	9.98	20.32	18.26	5	9
51	30	SK	25	27	-11	157.86	162.84	14.22	21.98	26.37	5	9
79	41	EB	19	22	0	195.74	199.79	11.55	17.92	17.92	5	9
87	42	EB	37	11	4	82.08	91.31	25.98	43.78	29.79	5	9
89	43	EB	4	25	0	290.45	293.20	7.84	13.35	13.35	5	9
35	27	SK	31	13	0	119.97	126.46	18.44	22.06	22.06	5.5	9
54	30	SK	21	26	-12	183.11	187.43	12.32	17.86	21.92	5.5	9
13	21	SK	17	23	-15	208.37	212.17	10.87	13.01	17.40	6	9
27	23	SK	30	12	0	126.28	132.47	17.58	20.50	20.50	6	9
32	24	RH	35	14	10	94.71	102.81	22.90	75.08	28.27	6	9
44	28	SK	3	41	-14	296.77	299.45	7.68	20.41	22.49	6	9
59	31	SK	26	27	0	151.54	156.73	14.79	27.49	27.49	6	9
80	41	EB	28	18	0	138.91	144.56	16.06	22.09	22.09	6	9
90	43	EB	25	17	0	157.86	162.84	14.22	18.93	18.93	6	9
92	43	EB	36	8	7	88.40	97.03	24.35	ERR	26.20	6	9
93	43	EB	30	16	5	126.28	132.47	17.58	30.79	22.81	6	9
1	20	RH	5	48	-15	284.14	286.94	8.01	27.55	29.71	7	9
2	20	RH	7	36	-15	271.51	274.44	8.38	18.21	20.81	7	9
5	20	SK	-4	36	-15	340.97	343.31	6.69	14.47	16.50	7	9
14	21	SK	14	35	-15	227.31	230.80	9.98	20.92	24.12	7	9

Table A-2. Pilot Rating Data and Effective Flight Path Angle Calculations (Sorted by HQR) - (Concluded)

APP #	FLIGHT	PILOT	DEPS	VDH	WIND	R	RS	GAMAF	GAMAEFF	NWGAMAEFF	HQR	GS ANGLE
20	23	RH	0	43	0	315.71	318.24	7.22	22.54	22.54	7	9
24	23	SK	-2	45	0	328.34	330.77	6.95	23.11	23.11	7	9
29	24	RH	14	37	6.5	227.31	230.80	9.98	28.20	25.87	7	9
33	24	SK	19	32	10	195.74	199.79	11.55	30.98	25.31	7	9
34	24	SK	7	41	10	271.51	274.44	8.38	27.62	24.67	7	9
36	27	SK	5	8	0	284.14	286.94	8.01	8.59	8.59	7	9
37	27	SK	35	14	0	94.71	102.81	22.90	28.27	28.27	7	9
42	28	SK	18	34	-15	202.06	205.98	11.20	22.60	26.30	7	9
43	28	SK	33	33	-11	107.34	114.55	20.44	43.37	50.43	7	9
45	28	SK	34	31	-12	101.03	108.66	21.60	41.42	49.50	7	9
56	31	SK	28	35	0	138.91	144.56	16.06	40.74	40.74	7	9
61	32	SK	4	40	0	290.45	293.20	7.84	22.24	22.24	7	9
70	37	MM	-3	47	-27	334.65	337.04	6.82	24.17	24.17	7	9
73	37	MM	23	36	-25	170.48	175.11	13.21	33.83	33.83	7	9
75	37	MM	25	32	-22	157.86	162.84	14.22	24.40	31.64	7	9
78	41	EB	-4	32	0	340.97	343.31	6.69	14.41	14.41	7	9
83	42	EB	34	26	8	101.03	108.66	21.60	51.73	40.10	7	9
84	42	EB	15	33	9	221.00	224.59	10.26	27.25	23.15	7	9
86	42	EB	10	38	0	252.57	255.72	9.00	24.01	24.01	7	9
88	42	EB	-1	40	4	322.03	324.50	7.08	20.83	20.00	7	9
91	43	EB	44	6	9	37.89	55.09	46.56	44.04	49.03	7	9
94	43	EB	24	23	3	164.17	168.97	13.69	24.19	22.06	7	9
31	24	RH	-2	45	11	328.34	330.77	6.95	25.54	23.11	8	9
57	31	SK	20	49	0	189.43	193.60	11.92	49.17	49.17	9	9
58	31	SK	22	62	0	176.80	181.27	12.75	ERR	ERR	9	9
95	39	SK	10	21	3	380.60	382.70	6.00	9.96	8.95	2.5	6
97	39	SK	17	30	0	314.00	316.53	7.26	14.62	14.62	3	6
100	39	SK	29	22	0	199.82	203.78	11.32	17.56	17.56	3	6
101	39	SK	25	25	0	237.88	241.22	9.55	16.31	16.31	3	6
102	39	SK	26	12	0	228.36	231.84	9.94	11.54	11.54	4.5	6
103	40	SK	-25	51	-4	713.63	714.75	3.21	12.32	12.55	4.5	6
98	39	SK	34	8	0	152.24	157.41	14.72	15.79	15.79	5	6
99	39	SK	17	19	0	314.00	316.53	7.26	10.19	10.19	5	6
96	39	SK	34	16	4	152.24	157.41	14.72	23.96	19.04	6	6
104	40	SK	36	27	-4	133.21	139.09	16.71	28.96	31.34	7	6
105	40	SK	0	47	-4	475.75	477.43	4.81	16.41	16.80	7	6
106	40	SK	32	4	-4	171.27	175.88	13.15	6.81	13.38	7	6
107	40	SK	30	35	-4	190.30	194.46	11.87	27.67	29.02	7	6
114	25	RH-FOG	12	20	-4	239.94	243.25	9.47	12.14	13.73	3	9
116	26	SK-FOG	5	20	-6	284.14	286.94	8.01	9.74	11.61	3	9
122	26	RH-FOG	7	22	-6	271.51	274.44	8.38	11.13	12.94	3	9
123	26	RH-FOG	2	10	-6	303.08	305.71	7.52	5.54	8.36	3	9
112	25	RH-FOG	21	20	-4	183.11	187.43	12.32	15.85	17.94	4	9
119	26	SK-FOG	11	12	-6	246.25	249.48	9.23	7.63	10.72	4.5	9
113	25	RH-FOG	13	32	-4	233.63	237.03	9.72	19.99	21.12	5	9
118	26	SK-FOG	6	10	-6	277.83	280.69	8.19	6.03	9.11	5	9
117	26	SK-FOG	0	33	-6	315.71	318.24	7.22	14.97	16.11	5.5	9
124	26	RH-FOG	18	21	-6	202.06	205.98	11.20	14.27	16.81	5.5	9
109	25	SK-FOG	4	30		290.45	293.20	7.84	14.87	15.82	6	9
110	25	SK-FOG	19	20		195.74	199.79	11.55	14.84	16.80	6	9
111	25	SK-FOG	15	11	,	221.00	224.59	10.26	8.91	11.65	6	9
115	25	RH-FOG	6	32	-4	277.83	280.69	8.19	16.78	17.72	6	9
120	26	RH-FOG	7	33	-6	271.51	274.44	8.38	17.43	18.77	6	9
108	25	SK-FOG	19	21	-4	195.74	199.79	11.55	15.46	17.35	7	9
121	26	RH-FOG	-6	46	-6	353.60	355.85	6.45	21.30	22.10	8	9

APPENDIX B

DERIVATION AND DISCUSSION OF EFFECTIVE FLIGHT PATH ANGLE

As discussed in Section II, the effective flight path angle concept has been used previously to study the effect of wind shear on powered lift STOL aircraft (see Ref. 5). The following formulation expands the Ref. 5 definition to larger angles.

The acceleration along the flight path may be expressed as,

$$a_x = \frac{dV_a}{dt} + g \sin \gamma_a \qquad (1)$$

Where V_a is the inertial velocity with respect to the airmass. Note that for a constant wind, the magnitude of the derivative of the inertial and airmass velocities is the same. The wind between decision-height and hover is assumed to be constant in this derivation, and the effect of windshear is considered to be an extension of the present work. Equation 1 is illustrated in Figure B-1a.

The effective flight path angle is defined as the flight path angle that will result in the same total acceleration as an aircraft operating at a constant airspeed, i.e., all the acceleration is due to the gravity term. This allows one to analyze the ability of the aircraft to simultaneously accelerate (or decelerate) and climb (or descend) in terms of the steady state γ - V performance curves (as discussed at length in Section III). Hence γ_a is equal to γ_{eff} when the dV_a/dt term is zero so that:

$$a_x = g \sin \gamma_{eff} \qquad (2)$$

Equating the two expressions for a_x,

$$\sin \gamma_{eff} = \frac{1}{g}\left(\frac{dV_a}{dt}\right) + \sin \gamma_a \qquad (3)$$

For a constant deceleration from decision-height to hover,

$$\Delta V_a^2 = V_{GS}^2 = 2 \frac{dV_a}{dt} R_s \qquad (4)$$

Where R_S is the slant range from decision-height to hover (see Figure B-1b). The change in speed between decision-height and hover must be the groundspeed at DH, since the speed at hover is, by definition, zero. Using equation 4 in equation 3, results in an expression for the effective flight path angle in terms of the range to hover and the aerodynamic flight path angle required to transition from DH to hover,

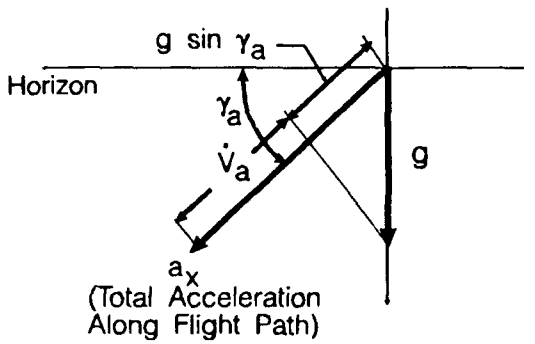

a) Acceleration Along Flight Path

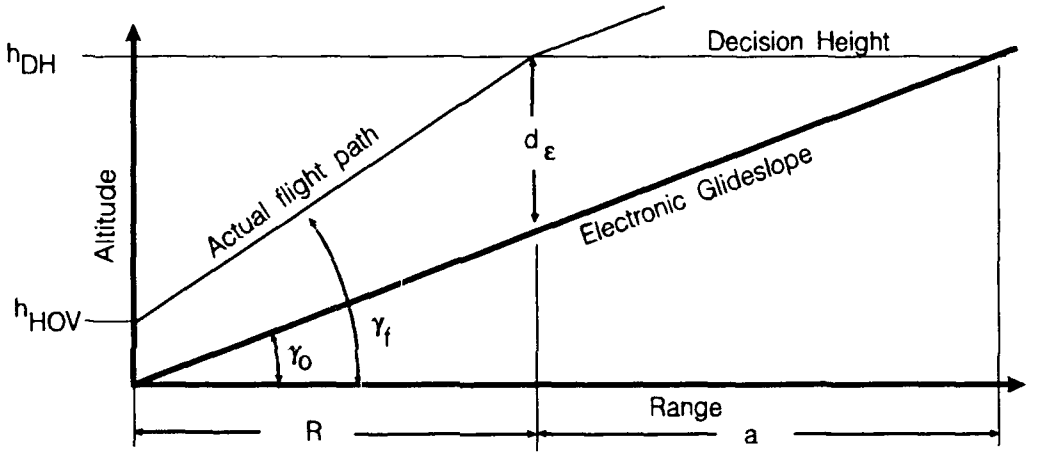

b) Geometry Between Decision-Height and Hover

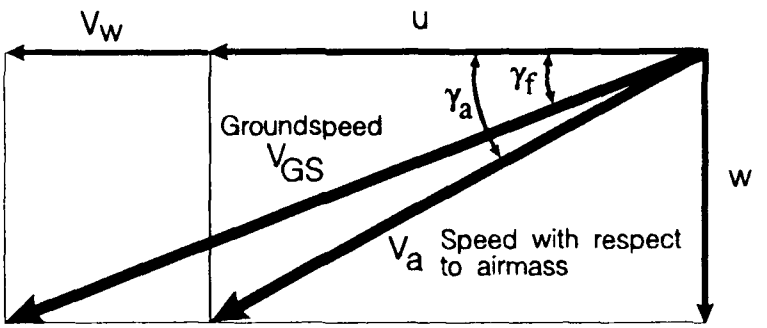

c) Relationship Between Airspeed and Groundspeed

Figure B-1 Kinematics Used to Define Effective Flight Path Angle

$$\sin\gamma_{eff} = \frac{V_{DH}^2}{2gR_s} + \sin\gamma_a \qquad (5)$$

For zero wind, the aerodynamic flight path angle, γ_a, is equal to the geometric (final) flight path angle, γ_f (see Figures B-1b and c). The effect of wind is to change the aerodynamic flight path angle as follows.

$$\sin\gamma_a = \frac{w}{V_a} \quad (see Figure\ B\text{-}1c)$$

$$V_a = \sqrt{(V_{DH}\cos\gamma_f - V_w)^2 + (V_{GS}\sin\gamma_f)^2}$$

$$\sin\gamma_a = \frac{V_{GS}\sin\gamma_f}{\sqrt{V_{GS}^2 + V_w^2 - 2V_{GS}V_w\cos\gamma_f}} \qquad (6)$$

Substituting equation 6 into equation 5,

$$\sin\gamma_{eff} = \frac{V_{DH}^2}{2gR_s} + \frac{V_{DH}\sin\gamma_f}{\sqrt{V_{DH}^2 + V_w^2 - 2V_{DH}V_w\cos\gamma_f}} \qquad (7)$$

This equation and the following expressions were used to calculate the values of effective flight path angle shown in Tables A-1 and A-2 in Appendix A.

$$Range = R = \frac{(h_{DH} - d_e)}{\tan\gamma_a} \quad (see\ Figure\ B\text{-}1b)$$

$$R_s = \sqrt{R^2 + (h_{DH} - h_{HOV})^2}$$

$$\sin\gamma_f = \frac{h_{DH} - h_{HOV}}{R_s}$$

$$\cos\gamma_f = \frac{R}{R_s}$$

The approximation in Figure 3 was obtained by assuming that the slant range is equal to the horizontal distance ($R_s \approx R$) and that $\cos\gamma_f \approx 1$, and $\sin\gamma_f \approx \gamma_f$. From Table A-1, it can be seen that these are very good approximations for the cases that were run in the flight test experiment. The extrapolations to larger glideslope angles in Section VId utilized the more exact expressions noted above.

☆U.S. GOVERNMENT PRINTING OFFICE: 1991 - 504-061/40041